PHYSICAL REVIEW D VOLUME 50, NUMBER 3 1 AUGUST 1994

Anomalous nuclear enhancement in deeply inelastic scattering and photoproduction

Ma Luo,[1] Jianwei Qiu,[1] and George Sterman[2]
[1]Department of Physics and Astronomy, Iowa State University, Ames, Iowa 50011
[2]Institute for Theoretical Physics, State University of New York, Stony Brook, New York 11794-3840
(Received 8 February 1994)

We derive the anomalous nuclear dependence of jet cross sections in deeply inelastic scattering and photoproduction, in terms of twist-four parton distributions in nuclei. This paper presents details of the use of factorization at higher twist to describe multiple scattering in nuclei, and the methods described here are applicable to a variety of other high-p_T cross sections.

PACS number(s): 13.60.Hb, 13.87.−a, 24.85.+p, 25.20.Lj

I. INTRODUCTION

Hard scattering in a nuclear environment affords challenging tests for the theory of strong interactions. Some time ago [1], it was observed that nuclear size effects are observable for momentum transfers hard enough to show partonic substructure [2]. By now, there is extensive experimental data on nuclear effects in exclusive scattering [3], single-particle inclusive hadroproduction [4], Drell-Yan, charmonium, and Υ production [5], jet hadroproduction [6,7], inclusive deeply inelastic scattering [8], and most recently, jet photoproduction [9] and jet production in deeply inelastic scattering [10]. On the theoretical side, considerable attention has been given to exclusive processes and possible nuclear transparency [11], as a test of the structure of both individual hadrons and nuclei, and to shadowing, as a probe of soft-parton evolution [12]. In contrast to shadowing, single-particle inclusive and jet production experiments often show a nuclear enhancement, in which the cross section rises faster than linearly with atomic number A. This effect was early on recognized as a sign of multiple scattering [13–15].

In our previous work [16], we showed that nuclear, enhancement in photoproduction may be brought directly into the scattering formalism of QCD, by treating it as a factorizable [17,18] nonleading-power correction to hard scattering [19]. Nuclear enhancement appears in this context as a property of two-parton matrix elements [16,20–22]. In this paper, we shall describe the details that led to our previous conclusions [16] and extend our results to jet cross sections in deeply inelastic scattering. We have recently [21] used jet photoproduction data to estimate the size of the relevant twist-four matrix elements. We reserve for future work applications to yet more complex processes, such as jet production in hadron-nucleus collisions, which involve initial-state strong interactions that are absent in deeply inelastic scattering and photoproduction.

Our basic observation that makes these developments possible is the following. The infrared divergences associated with soft rescatterings in perturbation theory may systematically be absorbed into higher-twist matrix elements, leaving behind calculable hard scattering functions. The reasoning that underlies this conclusion is described in some detail in Ref. [18].

We begin (Sec. II) with a review of the kinematics of jet production in deeply inelastic scattering (DIS). In Sec. III, we go on to describe how to isolate nonleading-power corrections in these processes by a "collinear expansion" in the momenta of the partons that participate in the hard process [17,21,22]. Section IV describes the calculation of the resulting DIS infrared-safe hard scattering functions at lowest order. We shall see that these contributions are proportional to new nuclear matrix elements, which differ from the quark and gluon distributions that occur at leading power by two extra gluonic field strengths, associated with the soft rescattering of outgoing partons. We will also identify the origin of nuclear size effects in the incomplete cancellation of final-state interactions at higher twist. Section V describes another effect, in which there are two sequential hard scatterings. This process is present in DIS although not in photoproduction. We note that at lowest order soft rescattering and double hard scattering occur for kinematically distinct parton momenta and contribute additively, without overlap. In Sec. VI, we discuss in more detail the origin of the A dependence in the matrix elements that we have derived. Section VII treats the reduction to photoproduction, and finally, Sec. VIII describes some details of practical calculations and our phenomenological results.

II. KINEMATICS

In most of the following discussion, we will study electron-nucleus DIS

$$e(L)\to e(L')+\gamma^*(q)\ , \tag{1a}$$

$$\gamma^*(q)+N(P_A)\to \text{jet}(l)+X\ . \tag{1b}$$

This semiinclusive process is pictured in Fig. 1. For kinematics, we rely on the analysis of Ref. [23]. We choose a frame in which the time component of the virtual photon momentum is zero and its space component lies along the negative z axis:

$$q^\mu=(0,0,0,-Q)\ , \tag{2}$$

where

0556-2821/94/50(3)/1951(21)/$06.00

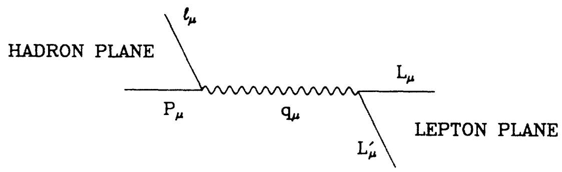

FIG. 1. Kinematics for semiinclusive one-jet production in lepton-hadron DIS.

$$Q^2=-q^2 . \tag{3}$$

The space components of the momentum of the incoming nucleon are along the positive z axis,

$$P^\mu=(P,0,0,P) , \tag{4}$$

and the nucleus has momentum

$$P_A{}^\mu=AP^\mu , \tag{5}$$

with A the atomic number.

In light-cone coordinates, we have

$$q^+=\frac{1}{\sqrt{2}}(q^0+q^z)=\frac{-Q}{\sqrt{2}} , \tag{6a}$$

$$q^-=\frac{1}{\sqrt{2}}(q^0-q^z)=\frac{Q}{\sqrt{2}} , \tag{6b}$$

$$\mathbf{q}_\perp=\mathbf{0}_\perp , \tag{6c}$$

or

$$q^\mu=\left[\frac{-Q}{\sqrt{2}},\frac{Q}{\sqrt{2}},\mathbf{0}_\perp\right] \tag{7}$$

and

$$P^\mu=(P^+,0,\mathbf{0}_\perp) \text{ with } P^+\equiv\sqrt{2}P . \tag{8}$$

The momentum of the observed final-state parton, l^μ, can be given as

$$l^\mu=\left[\frac{l_\perp^2}{2l^-},l^-,\mathbf{l}_\perp\right] , \tag{9}$$

consistent with $l^2=0$, where we fix its minus component l^- and transverse components $\mathbf{l}_\perp$. In this paper we are only concerned with larger $l_\perp^2$. The incident and final leptonic momenta L^μ and L'^μ are related by

$$q^\mu=L^\mu-L'^\mu , \tag{10a}$$

$$(L)^2=0 , \tag{10b}$$

$$(L')^2=0 , \tag{10c}$$

so that

$$2L\cdot q=-Q^2 . \tag{11}$$

This leads to

$$L^+=\left[\frac{Q^2}{2}\right]^{1/2}\left[\frac{w}{2P\cdot q}-1\right] , \tag{12a}$$

$$L^-=\left[\frac{Q^2}{2}\right]^{1/2}\frac{w}{2P\cdot q} , \tag{12b}$$

$$L^x=\sqrt{2L^+L^-}\cos\phi , \tag{12c}$$

$$L^y=\sqrt{2L^+l^-}\sin\phi , \tag{12d}$$

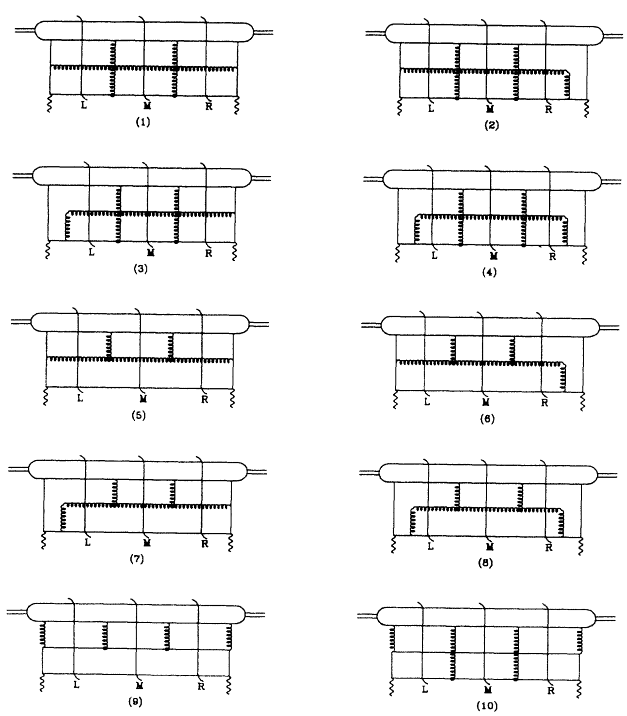

FIG. 2. Leading-order cut diagrams for soft rescattering in lepton-hadron DIS. L, M, and R stand for three possible cuts: left, middle, and right, respectively.

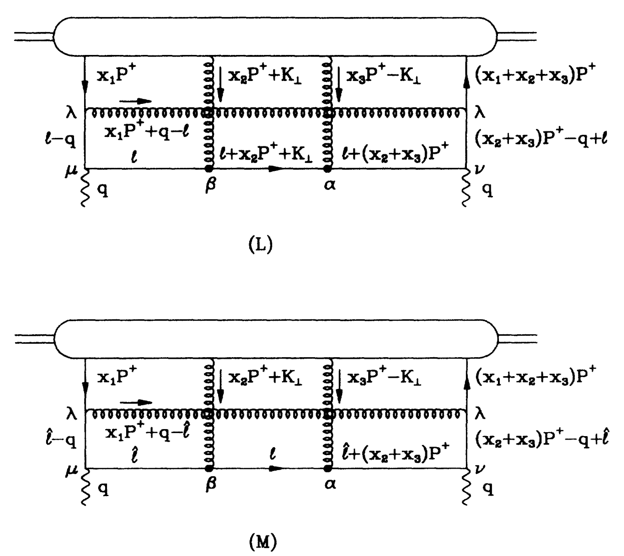

FIG. 3. Cut diagram in Fig. 2, diagram (1), with detailed labeling of parton momenta. The quark line of momentum l becomes a jet or fragments into an observed particle. A cut through the right (R) in this diagram is not shown.

where

$$w = 2(P \cdot L) \tag{13}$$

is related to the angle between **P** and **L**, while ϕ is the azimuthal angle between $\mathbf{L}_\perp$ and $l_\perp$, with $l_\perp$ chosen to lie along the x axis.

We are now ready to describe the basic processes at the partonic level that lead to nuclear enhancement.

III. COLLINEAR EXPANSION FOR ADDITIONAL SOFT SCATTERING

There are two sorts of double scattering processes that contribute to nuclear enhancement in DIS. The first is double hard scattering, which has been studied previously [13,14], although from a somewhat different point of view from the one we will take below. More details about our treatment of double hard scattering will be given in Sec. V. In the second sort of double scattering process, the large momentum transfer occurs in a single hard scattering, but an outgoing high-p_T parton absorbs a soft gluon, which modifies the overall cross section, without bringing in a large additional momentum. We will refer to this process as *soft rescattering* below and will concentrate on it first.

At lowest order, the partonic cross section corresponding to soft rescattering includes ten diagrams, and each diagram has three *cuts*, labeled by L, M, and R, respectively, as shown in Fig. 2. By convention, a cut is identified by a vertical line through the propagators in the figure that represent the final state (referred to as *cut lines* below). Let us consider one of these figures, Fig. 2, diagram (1), in detail to show how the fomalism works.

The example is shown in Fig. 3. Its contribution to the cross section can be written as

$$E_{L'}\frac{d^3\sigma_{qg}}{dL'^3} = \frac{\alpha_{\rm EM}^2 e_q^2}{2\pi w}\int \frac{d^4 l}{(2\pi)^4}\frac{1}{Q^4}L_{\mu\nu}W^{\mu\nu} , \tag{14a}$$

$$L_{\mu\nu} = \mathrm{Tr}[\not{L}\gamma_\mu \not{L}'\gamma_\nu] , \tag{14b}$$

$$W^{\mu\nu} = \int \frac{d^4K_1}{(2\pi)^4}\int \frac{d^4K_2}{(2\pi)^4}\int \frac{d^4K_3}{(2\pi)^4}\int d^4z_1\int d^4z_2\int d^4z_3 e^{iK_1z_1}e^{iK_2z_2}e^{iK_3z_3} \times \mathrm{Tr}\{\hat{H}^{\mu\alpha\beta\nu}(K_1,K_2,K_3)\langle A|T[\bar{\psi}(z_1)A_\beta(z_2)A_\alpha(z_3)]\psi(0)|A\rangle\} , \tag{14c}$$

where $\alpha_{\rm EM}$ is the electromagnetic fine-structure constant, and l and q denote the observed parton momentum and the momentum transfer, as above. For brevity, we will simplify for now to the case of one quark flavor, with electric charge e_q in units of electron charge. In Sec. VIII, we will return to the realistic case of multiple quark flavors. The momenta K_1, K_2, and K_3 are marked in Fig. 3. In Eq. (14c), $\hat{H}^{\mu\alpha\beta\nu}$ corresponds to the hard subprocess. ψ is the quark field and A_α the gluon field. We suppress color indices, which may be handled in a straightforward manner [21].

To pick up the leading contributions to the nuclear enhancement, we expand the parton momenta at the following values:

$$K_1 = x_1P^+\bar{n} , \tag{15a}$$

$$K_2 = x_2P^+\bar{n} + \mathbf{K}_{2\perp} , \tag{15b}$$

$$K_3 = x_3P^+\bar{n} + \mathbf{K}_{3\perp} . \tag{15c}$$

This is known as a *collinear expansion* [22,17]. The minus components of the K_i give even smaller contributions in $\hat{H}$ and will be neglected. In addition, $K_{1\perp}$ dependence in $\hat{H}$ will not be associated with A enhancement and we drop it as well. Later, we will show that x_2 and x_3 can be fixed by poles as functions of $\mathbf{K}_{2\perp}$ (or $\mathbf{K}_{3\perp}$) and $l_\perp$, and that they vanish when $K_{2\perp}$ and $K_{3\perp}$ go to zero.

Once we have dropped the $K_{1\perp}$ and K_i^- ($i=1,2,3$) dependence in $\hat{H}$, their integrals give δ functions and allow us rewrite Eq. (14c) as

$$W^{\mu\nu} = \int \frac{P^+dx_1}{2\pi}\int \frac{P^+dx_2}{2\pi}\frac{d^2K_{2\perp}}{(2\pi)^2}\int \frac{P^+dx_3}{2\pi}\frac{d^2K_{3\perp}}{(2\pi)^2}\int dz_1^- dz_2^- d^2z_{2\perp}dz_3^- d^2z_{3\perp} \times e^{ix_1P^+z_1^-}e^{ix_2P^+z_2^-}e^{-iK_{2\perp}\cdot z_{2\perp}}e^{ix_3P^+z_3^-}e^{-iK_{3\perp}\cdot z_{3\perp}} \times \mathrm{Tr}[\hat{H}^{\mu\alpha\beta\nu}(x_1P^+,K_2,K_3)\langle A|\bar{\psi}(z_1)A_\beta(z_2)A_\alpha(z_3)\psi(0)|A\rangle] . \tag{16}$$

Here we drop the time-ordering symbol, because eventually these fields will be restricted to the light cone, where they commute [18]. We now apply the collinear expansion as follows.

First of all, we expand the hard part in momenta about the collinear direction:

$$\hat{H}^{\mu\alpha\beta\nu}(x_1P^+,K_2,K_3)=\hat{H}^{\mu\alpha\beta\nu}(x_1P^+,x_2P^+,x_3P^+)+\left.\frac{\partial\hat{H}^{\mu\alpha\beta\nu}(x_1P^+,K_2,x_3P^+)}{\partial K_{2\rho}}\right|_{\mathbf{K}_{2\perp}=0_\perp}(K_2-x_2P^+)_\rho$$
$$+\left.\frac{\partial\hat{H}^{\mu\alpha\beta\nu}(x_1P^+,x_2P^+,K_3)}{\partial K_{3\sigma}}\right|_{\mathbf{K}_{3\perp}=0_\perp}(K_3-x_3P^+)_\sigma$$
$$+\frac{1}{2}\left.\frac{\partial^2\hat{H}^{\mu\alpha\beta\nu}(x_1P^+,K_2,K_3)}{\partial K_{2\rho}\partial K_{3\sigma}}\right|_{\mathbf{K}_{2\perp}=\mathbf{K}_{3\perp}=0_\perp}(K_2-x_2P^+)_\rho(K_3-x_3P^+)_\sigma+\cdots\ , \tag{17}$$

where we did not list explicitly terms such as $\partial^2\hat{H}^{\mu\alpha\beta\nu}/\partial K_{2\rho}^2$ and $\partial^2\hat{H}^{\mu\alpha\beta\nu}/\partial K_{3\sigma}^2$, because, for reasons that will become clear below, they do not contribute physical double scattering. We will return to this point at the end of this section. The factor $(K_i-x_iP^+)_\rho$ in Eq. (17) can be written as

$$(K_i-x_iP^+)_\rho=\omega_\rho^{\ \rho'}K_{i\rho'}\ , \tag{18}$$

with

$$\omega_\rho^{\ \rho'}=g_\rho^{\ \rho'}-\frac{P_\rho n^{\rho'}}{P\cdot n}\ . \tag{19}$$

In this discussion we will confine ourselves to experiments with unpolarized beams. Thus odd-twist contributions, e.g., the second and third terms in Eq. (17), vanish on taking a spin average. In addition, the leading term, $\hat{H}^{\mu\alpha\beta\nu}(x_1P^+,x_2P^+,x_3P^+)$ does not contribute to A enhancement because it is independent of transverse momenta. Later, in Sec. IV C, we will come back to this point in detail.

Next, by using

$$A_\alpha=\omega_\alpha^{\ \alpha'}A_{\alpha'}+P_\alpha\frac{A\cdot n}{P\cdot n}\ , \tag{20}$$

we expand the matrix element in the vector field components,

$$\langle A|\bar{\psi}(y_1^-)A_\beta(z_2)A_\alpha(z_3)\psi(0)|A\rangle=\omega_\alpha^{\ \alpha'}\omega_\beta^{\ \beta'}\langle A|\bar{\psi}(y_1^-)A_{\beta'}(z_2)A_{\alpha'}(z_3)\psi(0)|A\rangle$$
$$+\omega_\alpha^{\ \alpha'}\frac{P_\beta}{P\cdot n}\langle A|\bar{\psi}(y_1^-)n\cdot A(z_2)A_{\alpha'}(z_3)\psi(0)|A\rangle$$
$$+\frac{P_\alpha}{P\cdot n}\omega_\beta^{\ \beta'}\langle A|\bar{\psi}(y_1^-)A_{\beta'}(z_2)n\cdot A(z_3)\psi(0)|A\rangle$$
$$+\frac{P_\alpha P_\beta}{(P\cdot n)^2}\langle A|\bar{\psi}(y_1^-)n\cdot A(z_2)n\cdot A(z_3)\psi(0)|A\rangle\ . \tag{21}$$

It will be shown at the end of Sec. VI that because of the requirement of Lorentz boost invariance for the matrix elements, in a covariant gauge, as is used in this paper [17,18], terms associated with $\omega_\alpha^{\ \alpha'}A_{\alpha'}(z_i)$ are suppressed by $1/P^+$ compared to those with $n\cdot A(z_i)$. This makes the last term in Eq. (21),

$$[P_\alpha P_\beta/(P\cdot n)^2]\langle A|\bar{\psi}(y_1^-)n\cdot A(z_2)n\cdot A(z_3)\psi(0)|A\rangle\ ,$$

the dominant one. Therefore, in such a gauge, nuclear enhancement comes entirely from the single term

$$W^{\mu\nu}=\frac{1}{2}\int\frac{P^+dx_1}{2\pi}\int\frac{P^+dx_2}{2\pi}\frac{d^2K_{2\perp}}{(2\pi)^2}\int\frac{P^+dx_3}{2\pi}\frac{d^2K_{3\perp}}{(2\pi)^2}\int dy_1^-dz_2^-d^2z_{2\perp}dz_3^-d^2z_{3\perp}$$
$$\times e^{ix_1P^+y_1^-}e^{ix_2P^+z_2^-}e^{-iK_{2\perp}\cdot z_{2\perp}}e^{ix_3P^+z_3^-}e^{-iK_{3\perp}\cdot z_{3\perp}}$$
$$\times\mathrm{Tr}\left[\left.\frac{\partial^2\hat{H}^{\mu\alpha\beta\nu}(x_1P^+,K_2,K_3)}{\partial K_{2\rho}\partial K_{3\sigma}}\right|_{\mathbf{K}_{2\perp}=\mathbf{K}_{3\perp}=0_\perp}\times\frac{P_\alpha P_\beta}{(P\cdot n)^2}\omega_\rho^{\ \rho'}K_{2\rho'}\omega_\sigma^{\ \sigma'}K_{3\sigma'}\times\langle A|\bar{\psi}(y_1^-)n\cdot A(z_2)n\cdot A(z_3)\psi(0)|A\rangle\right]\ . \tag{22}$$

To derive a factorized form for $W^{\mu\nu}$, we treat Eq. (22) in the following three steps.

(i) Ignoring the effect of twist higher than four, the Dirac trace in Eq. (22) can be separated into two,

$$\mathrm{Tr}\left[\frac{\partial^2 \hat{H}^{\mu\alpha\beta\nu}(x_1P^+,K_2,K_3)}{\partial K_{2\rho}\partial K_{3\sigma}}\Bigg|_{\mathbf{K}_{2\perp}=\mathbf{K}_{3\perp}=0_\perp}\langle A|\bar{\psi}(y_1^-)n\cdot A(z_2)n\cdot A(z_3)\psi(0)|A\rangle\right]$$
$$=\frac{1}{4(P\cdot n)}\frac{\partial^2}{\partial K_{2\rho}\partial K_{3\sigma}}\{\mathrm{Tr}[\hat{H}^{\mu\alpha\beta\nu}(x_1P^+,K_2,K_3)\not{P}]\}|_{\mathbf{K}_{2\perp}=\mathbf{K}_{3\perp}=0_\perp}\mathrm{Tr}[\langle A|\bar{\psi}(y_1^-)\not{n}n\cdot A(z_2)n\cdot A(z_3)\psi(0)|A\rangle]\ . \quad (23)$$

(ii) We integrate by parts in z_2 and z_3 to change the momenta $K_{2\rho'}$ and $K_{3\sigma'}$ into derivatives on fields, $\partial/\partial z_2^{\rho'}$ and $\partial/\partial z_3^{\sigma'}$,

$$\int d^2z_{2\perp}d^2z_{3\perp}e^{-iK_{2\perp}\cdot z_{2\perp}}e^{-iK_{3\perp}\cdot z_{3\perp}}\omega_\rho{}^{\rho'}K_{2\rho'}\omega_\sigma{}^{\sigma'}K_{3\sigma'}\mathrm{Tr}[\langle A|\bar{\psi}(y_1^-)\not{n}n\cdot A(z_2)n\cdot A(z_3)\psi(0)|A\rangle]$$
$$=\frac{1}{(-i)^2}\omega_\rho{}^{\rho'}\omega_\sigma{}^{\sigma'}\int d^2z_{2\perp}d^2z_{3\perp}e^{-iK_{2\perp}\cdot z_{2\perp}}e^{-iK_{3\perp}\cdot z_{3\perp}}\mathrm{Tr}\left[\langle A|\bar{\psi}(y_1^-)\not{n}\frac{\partial[n\cdot A(z_2)]}{\partial z_2^{\rho'}}\frac{\partial[n\cdot A(z_3)]}{\partial z_3^{\sigma'}}\psi(0)|A\rangle\right]\ . \quad (24)$$

(iii) The $\hat{K}_{2\perp}$ and $\hat{K}_{3\perp}$ integrals now only act on the exponential factors $e^{-iK_{2\perp}\cdot z_{2\perp}}e^{-iK_{3\perp}\cdot z_{3\perp}}$ and thus give δ functions. The result of these steps is

$$W^{\mu\nu}=-\frac{1}{8}\omega_\rho{}^{\rho'}\omega_\sigma{}^{\sigma'}\int\frac{dy_1^-}{2\pi}\frac{dy_2^-}{2\pi}\frac{dy_3^-}{2\pi}\int dx_1dx_2dx_3e^{ix_1P^+y_1^-}e^{ix_2P^+y_2^-}e^{ix_3P^+y_3^-}$$
$$\times\frac{\partial^2}{\partial K_{2\rho}\partial K_{3\sigma}}\{\mathrm{Tr}[\hat{H}^{\mu\alpha\beta\nu}(x_1P^+,K_2,K_3)\not{P}P_\alpha P_\beta]\}|_{\mathbf{K}_{2\perp}=\mathbf{K}_{3\perp}=0_\perp}$$
$$\times\mathrm{Tr}\left\{\left\langle A|\bar{\psi}(y_1^-)\not{n}\frac{\partial[n\cdot A(z_2)]}{\partial z_2^{\rho'}}\frac{\partial[n\cdot A(z_3)]}{\partial z_3^{\sigma'}}\psi(0)|A\right\rangle\right\}\Bigg|_{\substack{z_2=y_2^-\\z_3=y_3^-}}\ . \quad (25)$$

Because the values of x_1, x_2, and x_3 will be fixed by δ functions and poles of the hard part $\hat{H}^{\mu\alpha\beta\nu}(x_1P,K_2,K_3)$ (we will exhibit this shortly in Sec. IV), we move the exponentials and integrals $\int dx_1dx_2dx_3e^{ix_1P^+y_1^-}e^{ix_2P^+y_2^-}e^{ix_3P^+y_3^-}$ inside the derivative of $\partial^2/\partial K_{2\rho}\partial K_{3\sigma}$,

$$W^{\mu\nu}=-\frac{1}{8}\omega_\rho{}^{\rho'}\omega_\sigma{}^{\sigma'}\int\frac{dy_1^-}{2\pi}\frac{dy_2^-}{2\pi}\frac{dy_3^-}{2\pi}\mathrm{Tr}\left\{\langle A|\bar{\psi}(y_1^-)\not{n}\frac{\partial[n\cdot A(z_2)]}{\partial z_2^{\rho'}}\frac{\partial[n\cdot A(z_3)]}{\partial z_3^{\sigma'}}\psi(0)|A\rangle\right\}\Bigg|_{\substack{z_2=y_2^-\\z_3=y_3^-}}$$
$$\times\frac{\partial^2}{\partial K_{2\rho}\partial K_{3\sigma}}\left\{\int dx_1dx_2dx_3e^{ix_1P^+y_1^-}e^{ix_2P^+y_2^-}e^{ix_3P^+y_3^-}\right.$$
$$\left.\times\mathrm{Tr}[\hat{H}^{\mu\alpha\beta\nu}(x_1P^+,K_2,K_3)\not{P}P_\alpha P_\beta]\right\}\Bigg|_{\mathbf{K}_{2\perp}=\mathbf{K}_{3\perp}=0_\perp}\ . \quad (26)$$

Note that the derivatives act on the $K_\perp$ dependence in the exponentials as well, once the x_i integrals are carried out as contour integrations.

As mentioned above (see Sec. VI for more details), in a covariant gauge, terms with $\omega_\alpha{}^{\alpha'}A_{\alpha'}(z_i)$ are suppressed compared to those with $n\cdot A(z_i)$. So we have, keeping only the minimal number of fields,

$$\omega_\rho{}^{\rho'}F_{+\rho'}(y_2^-)\equiv\omega_\rho{}^{\rho'}\frac{\partial}{\partial z_2{}^{\rho'}}[n\cdot A(z_2)]|_{z_2=y_2^-}-\left[n\cdot\frac{\partial}{\partial z_2}\right][\omega_\rho{}^{\rho'}A_{\rho'}(z_2)]|_{z_2=y_2^-}$$
$$\approx\omega_\rho{}^{\rho'}\frac{\partial}{\partial z_2{}^{\rho'}}[n\cdot A(z_2)]|_{z_2=y_2^-}\ , \quad (27a)$$

$$\omega_\sigma{}^{\sigma'}F_{+\sigma'}(y_3^-)\equiv\omega_\sigma{}^{\sigma'}\frac{\partial}{\partial z_3{}^{\sigma'}}[n\cdot A(z_3)]|_{z_3=y_3^-}-\left[n\cdot\frac{\partial}{\partial z_3}\right][\omega_\sigma{}^{\sigma'}A_{\sigma'}(z_3)]\Bigg|_{z_3=y_3^-}$$
$$\approx\omega_\sigma{}^{\sigma'}\frac{\partial}{\partial z_3{}^{\sigma'}}[n\cdot A(z_3)]|_{z_3=y_3^-}\ . \quad (27b)$$

Then the matrix element in Eq. (26) becomes, up to power-suppressed corrections,

$$\langle A|\bar{\psi}(y_1^-)F_{+\rho'}(y_2^-)F_{+\sigma'}(y_3^-)\psi(0)|A\rangle\ . \quad (28)$$

In principle, we can expand matrix elements such as these as

$$\langle F_{+\rho'}(y_2^-)F_{+\sigma'}(y_3^-)\rangle = C_1\bar{n}_{\rho'}n_{\sigma'}+C_2 n_{\rho'}\bar{n}_{\sigma'}+C_3\bar{n}_{\rho'}\bar{n}_{\sigma'} + C_4 n_{\rho'}n_{\sigma'}+C_5 d_{\rho'\sigma'} , \quad (29)$$

where

$$d_{\rho'\sigma'}\equiv \bar{n}_{\rho'}n_{\sigma'}+n_{\rho'}\bar{n}_{\sigma'}-g_{\rho'\sigma'} . \quad (30)$$

Then we have

$$C_1=n^i\bar{n}^j\langle F_{+i}(y_2^-)F_{+j}(y_3^-)\rangle = \langle F_{++}F_{+-}\rangle=0 , \quad (31a)$$

$$C_2=\bar{n}^i n^j\langle F_{+i}(y_2^-)F_{+j}(y_3^-)\rangle = \langle F_{+-}F_{++}\rangle=0 , \quad (31b)$$

$$C_3=n^i n^j\langle F_{+i}(y_2^-)F_{+j}(y_3^-)\rangle = \langle F_{++}F_{++}\rangle=0 , \quad (31c)$$

$$C_4=\bar{n}^i\bar{n}^j\langle F_{+i}(y_2^-)F_{+j}(y_3^-)\rangle = \langle F_{+-}F_{+-}\rangle , \quad (31d)$$

$$C_5=\frac{d_{ij}}{2}\langle F_{+i}(y_2^-)F_{+j}(y_3^-)\rangle = \tfrac{1}{2}\langle F_{+\perp}(y_2^-)F_+{}^{\perp}(y_3^-)\rangle , \quad (31e)$$

where the expectation values are all in the nuclear state $|A\rangle$. For the $C_4 n_{\rho'}n_{\sigma'}$ term, we have

$$\omega_\rho{}^{\rho'}\omega_\sigma{}^{\sigma'}n_{\rho'}n_{\sigma'}\frac{\partial^2}{\partial K_{2\rho}\partial K_{3\sigma}}=\frac{\partial^2}{\partial K_2^-\partial K_3^-} .$$

Because of the approximation that $K_2^-=K_3^-=0$, i.e., Eqs. (15b) and (15c), the hard part $\hat{H}^{\mu\alpha\beta\nu}(x_1P^+,K_2,K_3)$ is independent of K_2^- and K_3^-. Thus

$$\frac{\partial^2}{\partial K_2^-\partial K_3^-}[\hat{H}^{\mu\alpha\beta\nu}(x_1P^+,K_2,K_3)]=0 ,$$

and the $C_4 n_{\rho'}n_{\sigma'}$ term vanishes in our approximations. Therefore, $W^{\mu\nu}$ turns out to be

$$W^{\mu\nu}=-\frac{1}{16}\int\frac{dy_1^-}{2\pi}\frac{dy_2^-}{2\pi}\frac{dy_3^-}{2\pi}\mathrm{Tr}[\langle A|\bar{\psi}(y_1^-)\not{n}F_{+\perp}(y_2^-)F_+{}^{\perp}(y_3^-)\psi(0)|A\rangle] \times\frac{\partial^2}{\partial K_{2\perp}\partial K_3^{\perp}}\left\{\int dx_1dx_2dx_3e^{ix_1P^+y_1^-}e^{ix_2P^+y_2^-}e^{ix_3P^+y_3^-} \times\mathrm{Tr}[\hat{H}^{\mu\alpha\beta\nu}(x_1P^+,K_2,K_3)\not{P}P_\alpha P_\beta]\right\}\Bigg|_{\mathbf{K}_{2\perp}=\mathbf{K}_{3\perp}=0_\perp} , \quad (32)$$

where we observe

$$\omega_\rho{}^{\rho'}\omega_\sigma{}^{\sigma'}d_{\sigma'\rho'}=d_{\sigma\rho} . \quad (33)$$

Equation (32) has been derived at lowest order in the hard scattering. As it stands, of course, it is not gauge invariant. Gauge invariance is incorporated at higher orders and leading power by taking into account diagrams involving more fields $n\cdot A$, which will form ordered exponentials between the physical fields shown in (32), as discussed, for instance, in [17]. Such fields, however, cannot correspond to physical rescatterings, since they can be eliminated by a change of gauge. This is the reason why we neglected terms in the collinear expansion [Eq. (17)] that involved two derivatives with respect to K_2 and none with respect to K_3, or vice versa. Such a term would involve only three physical fields instead of four. As we shall see in Sec. VI, four physical fields are required to produce nuclear enhancement.

IV. CALCULATION OF THE HARD PART

A. Combining cut diagrams

Now we are ready to discuss the calculation of the hard part,

$$T_{1-L}\equiv\int dx_1dx_2dx_3e^{ix_1P^+y_1^-}e^{ix_2P^+y_2^-}e^{ix_3P^+y_3^-} \times\mathrm{Tr}[\hat{H}^{\mu\alpha\beta\nu}(x_1P^+,K_2,K_3)\not{P}P_\alpha P_\beta] .$$

As an example, we still work with Fig. 3. In the following calculation, two important points should be anticipated.

First, as is shown in the diagram, after a hard scattering the outgoing parton interacts with two more soft gluons from the nucleus. Thus, in evaluating the cross section, we encounter one phase space δ function and two virtual propagators involving the x_i's. The poles of these propagators will fix x_2 and x_3 to be functions of the transverse momenta $K_{i\perp}$. Then the x_2 and x_3 will vanish in the limit $K_{i\perp}\to 0$. Therefore $e^{ix_2P^+y_3^-}$ and $e^{ix_3P^+y_3^-}$ will reduce to unity eventually. In the absence of y^--dependent phases, we may expect a significant contribution from the free integrals $\int dy_2^-dy_3^-$. This will be the origin of the A enhancement.

In addition we will find a cancellation by summing over the three cut diagrams, Figs. 3(L), 3(M), and 3(R), corresponding to final-state cuts on the left, middle, and right of the diagram in Fig. 3, respectively. This cancellation eliminates the twist-two and even some twist-four terms contained in Eq. (16). Nevertheless, certain twist-four terms will survive. Along with the lack of y^--dependent phases, this is another necessary condition for A enhancement.

In the case that the cut is on the left, as shown in Fig. 3(L), we have

$$\mathrm{Tr}[\hat{H}^{\mu\alpha\beta\nu}(x_1P^+,K_2,K_3)\not{P}P_\alpha P_\beta]$$
$$=-g^4\frac{\mathrm{Tr}\{\not{P}\gamma^\lambda[\not{l}+(x_2+x_3)\not{P}-\not{q}]\gamma^\nu[\not{l}+(x_2+x_3)\not{P}]}{(l-q)^2[l+(x_2+x_3)P^+-q]^2\{[l+(x_2+x_3)P^+]^2-i\varepsilon\}}$$
$$\times\frac{\not{P}(\not{l}+x_2\not{P}+\not{K}_\perp)\not{P}\not{l}\gamma^\mu(\not{l}-\not{q})\gamma_\lambda\}}{\{[l+x_2P^++K_\perp]^2-i\varepsilon\}}(2\pi)^2\delta_+(l^2)\delta_+[(x_1P^++q-l)^2]\,, \tag{34}$$

where we have taken $K_{2\perp}=-K_{3\perp}=K_\perp$ by momentum conservation. We now define

$$\Gamma^{\mu\nu}_{1-L}\equiv\frac{-1}{(l-q)^2[l+(x_2+x_3)P^+-q]^2}\mathrm{Tr}\{\not{P}\gamma^\lambda[\not{l}+(x_2+x_3)\not{P}-\not{q}]$$
$$\times\gamma^\nu[\not{l}+(x_2+x_3)\not{P}]\not{P}(\not{l}+x_2\not{P}+\not{K}_\perp)\not{P}\not{l}\gamma^\mu(\not{l}-\not{q})\gamma_\lambda\}\,, \tag{35}$$

where the index $1-L$ denotes that it belongs to the process shown in Fig. 3(L). $\Gamma^{\mu\nu}_{1-L}$ includes off-shell propagators only, and so it is a smooth function of the x_i's, which can be fixed by the relevant poles and the δ function. Once the values of the x_i have been fixed, $\Gamma^{\mu\nu}_{1-L}$ can be pulled out of the integrals $\int dx_1dx_2dx_3$ as a finite constant tensor. Thus $\Gamma^{\mu\nu}_{1-L}$ does not yield any A enhancement.

To get the cross section, we must compute 24 different $\Gamma^{\mu\nu}_{i-a}$, with $i=1$–8 and $a=L$, M, and R, each corresponding to an individual cut diagram shown in Fig. 2. To write them as symbols $\Gamma^{\mu\nu}_{1-a}$ instead of their full expressions in the text will be more convenient, since they do not play an important role in the A dependence. For all of the left-cut diagrams in Fig. 2, the remaining factors in $\mathrm{Tr}[\hat{H}^{\mu\alpha\beta\nu}\not{P}P_\alpha P_\beta]$, fortunately, have a common form. It includes two final-state δ functions, two propagators, which can go on shell, and three exponentials,

$$B\equiv(2\pi)^2\delta_+(l^2)\delta_+[(x_1P^++q-l)^2]$$
$$\times e^{ix_1P^+y_1^-}e^{ix_2P^+y_2^-}e^{ix_3P^+y_3^-}$$
$$\times\frac{1}{[l+(x_2+x_3)P^+]^2-i\varepsilon}$$
$$\times\frac{1}{[l+x_2P^++K_\perp]^2-i\varepsilon}\,. \tag{36}$$

As we shall see, the quantity B [Eq. (36)] controls the A enhancement with which we are concerned.

To evaluate Eq. (36), note that

$$\delta[(x_1P^++q-l)^2]=\frac{1}{s+t+Q^2}\delta\left[x_1+\frac{u}{s+t+Q^2}\right]\,, \tag{37a}$$

$$\frac{1}{[l+(x_2+x_3)P^+]^2-i\varepsilon}=\frac{1}{-t[(x_2+x_3)+i\varepsilon/t]}\,, \tag{37b}$$

$$\frac{1}{[l+x_2P^++K_\perp]^2-i\varepsilon}$$
$$=\frac{1}{-t\{x_2+[(K_\perp^2+2l_\perp\cdot K_\perp)/t+i\varepsilon/t]\}}\,, \tag{37c}$$

where

$$s\equiv(P+q)^2=2P^+q^--Q^2\,, \tag{38a}$$

$$t\equiv(P-l)^2=-2P^+l^-\,, \tag{38b}$$

$$u\equiv(l-q)^2\,. \tag{38c}$$

Now we can rewrite the integral $\int dx_1dx_2dx_3B\Gamma^{\mu\nu}_{1-L}$ as

$$\int_{-\infty}^{+\infty}dx_1dx_2dx_3B\Gamma^{\mu\nu}_{1-L}=\int_{-\infty}^{+\infty}dx_1dx_2d(x_2+x_3)\frac{(2\pi)^2}{2l^-}\delta\left[l^+-\frac{l_\perp^2}{2l^-}\right]\frac{1}{s+t+Q^2}\delta\left[x_1+\frac{u}{s+t+Q^2}\right]$$
$$\times\frac{e^{ix_1P^+y_1^-}e^{ix_2P^+(y_2^--y_3^-)}e^{i(x_2+x_3)P^+y_3^-}\Gamma^{\mu\nu}_{1-L}}{4t^2[(x_2+x_3)-i\varepsilon']\{x_2-[(-K_\perp^2+2l_\perp\cdot K_\perp)/t+i\varepsilon']\}}\,, \tag{39}$$

with

$$\varepsilon'\equiv\frac{\varepsilon}{2P^+l^-}>0\,. \tag{40}$$

We see that both variables x_2 and x_2+x_3 have poles in the upper half complex plane. So after fixing x_1 from $\delta(x_1+u/(s+t+Q^2))$, we can carry out the other integrals $\int dx_2dx_3$ by using contour integrations in x_2 and x_2+x_3, closing at infinity, and circling the poles, to get

$$T_{1-L}=\int dx_1dx_2dx_3 e^{ix_1P^+y_1^-}e^{ix_2P^+y_2^-}e^{ix_3P^+y_3^-}\,\mathrm{Tr}[\hat{H}^{\mu\alpha\beta\nu}_{1-L}(x_1P^+,K_2,K_3)\not{P}P_\alpha P_\beta]$$
$$=-g^4\int\frac{dx_1}{t^2}\frac{(2\pi)^4}{2l^-}\delta\left[l^+-\frac{l_\perp^2}{2l^-}\right]\frac{1}{(s+t+Q^2)}\delta\left[x_1+\frac{u}{s+t+Q^2}\right]\Gamma^{\mu\nu}_{1-L}$$
$$\times e^{ix_1P^+y_1^-}\exp\left[i\left[\frac{K_\perp^2+2K_\perp\cdot l_\perp}{2l^-}\right](y_2^--y_3^-)\right]\theta(y_2^--y_3^-)\theta(y_3^-)\bigg|_{x_2=x_2^0,\ x_3=x_3^0}, \tag{41}$$

where

$$x_2^0=-x_3^0=\frac{K_\perp^2+2K_\perp\cdot l_\perp}{-t}. \tag{42}$$

The Dirac trace of $\Gamma^{\mu\nu}_{1-L}$ includes a factor

$$[\not{l}+(x_2^0+x_3^0)\not{P}]\not{P}(\not{l}+x_2^0\not{P}+\not{K}_\perp)\not{P}\not{l}=t^2\not{l}. \tag{43}$$

A little algebra then gives

$$\Gamma^{\mu\nu}_{1-L}=\frac{2t^2\,\mathrm{Tr}[\not{P}(\not{l}-\not{q})\gamma^\mu\not{l}\gamma^\nu(\not{l}-\not{q})]}{u^2}. \tag{44}$$

We see that after the integrals of $\int dx_2dx_3$, for fixed P and q, $\Gamma^{\mu\nu}_{1-L}$ is a function of l only, so that we can denote $\Gamma^{\mu\nu}_{1-L}\equiv\Gamma^{\mu\nu}_1(l)$.

Figure 3(R), with the cut on the right, can be treated by a similar procedure. The essential difference is in the signs of the $i\varepsilon$'s and in the δ function. The δ function in $T^{\mu\nu}_{1-L}$ fixes $x_1=u/(s+t+Q^2)$, whereas the δ function in $T^{\mu\nu}_{1-R}$ fixes $x_1+x_2+x_3=u/(s+t+Q^2)$. This difference will consequently influence the pole structure in $T^{\mu\nu}_{1-R}$ and then make its θ functions in the y_i^- different from those in $T^{\mu\nu}_{1-L}$ [see Eq. (41)]. We find

$$T_{1-R}=\int dx_1dx_2dx_3 e^{ix_1P^+y_1^-}e^{ix_2P^+y_2^-}e^{ix_3P^+y_3^-}\,\mathrm{Tr}[\hat{H}^{\mu\alpha\beta\nu}_{1-R}(x_1P^+,K_2,K_3)\not{P}P_\alpha P_\beta]$$
$$=-g^4\int\frac{dx_1}{t^2}\frac{(2\pi)^4}{2l^-}\delta\left[l^+-\frac{l_\perp^2}{2l^-}\right]\frac{1}{(s+t+Q^2)}\delta\left[x_1+\frac{u}{s+t+Q^2}\right]\Gamma^{\mu\nu}_{1-R}$$
$$\times e^{ix_1P^+y_1^-}\exp\left[i\left[\frac{K_\perp^2+2K_\perp\cdot l_\perp}{2l^-}\right](y_2^--y_3^-)\right]\theta(y_3^--y_2^-)\theta(y_2^--y_1^-)\bigg|_{x_2=x_2^0,\ x_3=x_3^0}, \tag{45}$$

where x_2^0 and x_3^0 are the same as in T_{1-L}. It is easy to show that $\Gamma^{\mu\nu}_{1-R}=\Gamma^{\mu\nu}_{1-L}$, which is a function of l only, as shown in Eq. (44).

When the cut is through the middle [Fig. 3(M)], we have a slightly different result

$$T_{1-M}=\int dx_1dx_2dx_3 e^{ix_1P^+y_1^-}e^{ix_2P^+y_2^-}e^{ix_3P^+y_3^-}\,\mathrm{Tr}[\hat{H}^{\mu\alpha\beta\nu}_{1-M}(x_1P^+,K_2,K_3)\not{P}P_\alpha P_\beta]$$
$$=g^4\int\frac{d\hat{x}_1}{t^2}\frac{(2\pi)^4}{2l^-}\delta\left[l^+-\frac{l_\perp^2}{2l^-}\right]\frac{1}{(s+t+Q^2)}\delta\left[\hat{x}_1+\frac{\hat{u}}{s+t+Q^2}\right]\Gamma^{\mu\nu}_{1-M}$$
$$\times e^{i\hat{x}_1P^+y_1^+}\exp\left[i\left[\frac{K_\perp^2-2K_\perp\cdot l_\perp}{2l^-}\right](y_3^--y_2^-)\right]\theta(y_2^--y_1^-)\theta(y_3^-)\bigg|_{x_2=\hat{x}_2^0,\ x_3=\hat{x}_3^0}, \tag{46}$$

where

$$\hat{x}_1=x_1-\hat{x}_2^0, \tag{47a}$$
$$\hat{x}_2^0=-\hat{x}_3^0=\frac{K_\perp^2-2K_\perp\cdot l_\perp}{t}, \tag{47b}$$
$$\hat{l}=l-x_2^0P^+-K_\perp, \tag{47c}$$
$$\hat{u}=(\hat{l}-q)^2. \tag{47d}$$

The differences in the θ functions between (41), (45), and (46), and in the exponential of T_{1-M} relative to T_{1-L} and T_{1-R}, result from differences in the phase space δ functions and in the pole structure of the x_i's between the three T's. Moreover, it is easy to find that $\Gamma^{\mu\nu}_{1-M}$ is also given by Eq. (44), apart from replacing the l with $\hat{l}$, i.e., $\Gamma^{\mu\nu}_{1-M}(l)=\Gamma^{\mu\nu}_{1-L}(l\to\hat{l})\equiv\Gamma^{\mu\nu}_1(\hat{l})$.

B. $K_\perp$ expansion

At this stage, we are ready to expand T_{1-L}, T_{1-M}, and T_{1-R} in $K_\perp$ to make contact with the general factorized expression Eq. (32). To do so, we need first to expand the exponentials in T_{1-L} [Eq. (41)] and T_{1-R} [Eq. (45)],

$$\exp\left[i\left[\frac{K_\perp^2+2K_\perp\cdot l_\perp}{2l^-}\right](y_2^- - y_3^-)\right],$$

and in T_{1-M} [Eq. (46)],

$$\exp\left[i\left[\frac{K_\perp^2-2K_\perp\cdot l_\perp}{2l^-}\right](y_3^- - y_2^-)\right].$$

In both cases the linear term in the Taylor expansion gives a matrix element

$$\int dy_2^- dy_3^- \langle A|F(y_2^-)F(y_3^-)|A\rangle (y_2^- - y_3^-) = \tfrac{1}{2}\int dv \int du \langle A|F(u)F(0)|A\rangle u, \quad (48)$$

where $u=y_2^- - y_3^-$, $v=y_2^- + y_3^-$, and we omit the ψ fields and indices of the F's. This term [Eq. (48)] may be eliminated by using the fact that the fields commute on the light cone [18]. In other words, on the light cone we have

$$\langle A|F(u)F(0)|A\rangle = \langle A|F(0)F(u)|A\rangle = \langle A|F(-u)F(0)|A\rangle,$$

so that

$$\int_{-\infty}^{+\infty} du \langle A|F(u)F(0)|A\rangle u = -\int_{-\infty}^{+\infty} du \langle A|F(u)F(0)|A\rangle u = 0.$$

Up to terms that vanish faster than $K_\perp^2$, we may therefore replace $\exp[i((K_\perp^2-2K_\perp\cdot l_\perp)/2l^-)(y_3^- - y_2^-)]$ by $\exp[i((K_\perp^2+2K_\perp\cdot l_\perp)/2l^-)(y_2^- - y_3^-)]$ in T_{1-M}, which makes the exponentials in the three T's the same.

We can now combine the three cut diagrams of Fig. 3 to get

$$\begin{aligned} T_{1-L}+T_{1-M}+T_{1-R} = &-g^4\int \frac{dx_1}{t^2}\frac{(2\pi)^4}{2l^-}\delta\left[l^+ - \frac{l_\perp^2}{2l^-}\right]\frac{1}{(s+t+Q^2)}e^{ix_1p^+y_1^+} \\ &\times\left\{\Gamma_{1-L}^{\mu\nu}\delta\left[x_1+\frac{u}{s+t+Q^2}\right]\exp\left[i\left[\frac{K_\perp^2+2K_\perp\cdot l_\perp}{2l^-}\right](y_2^- - y_3^-)\right]\right. \\ &\times[\theta(y_2^- - y_3^-)\theta(y_3^-)+\theta(y_3^- - y_2^-)\theta(y_2^- - y_1^-)-\theta(y_2^- - y_1^-)\theta(y_3^-)] \\ &\left.+\left[\Gamma_{1-L}^{\mu\nu}\delta\left[x_1+\frac{u}{s+t+Q^2}\right]-\Gamma_{1-M}^{\mu\nu}\delta\left[x_1+\frac{\hat{u}}{s+t+Q^2}\right]\right]\theta(y_2^- - y_1^-)\theta(y_3^-)\right\}, \end{aligned} \quad (49)$$

where we have taken $\Gamma_{1-L}^{\mu\nu}=\Gamma_{1-R}^{\mu\nu}$, as is noted before. The exponential in $K_\perp$ is suppressed in the final line, because it only contributes at the order of $K_\perp^3$. Corrections to Eq. (49) are either further power suppressed or lack A enhancement.

C. Origin of A enhancement

Let us now study the range of the y_i^- integrals in Eq. (49). The factor

$$[\theta(y_2^- - y_3^-)\theta(y_3^-)+\theta(y_3^- - y_2^-)\theta(y_2^- - y_1^-)-\theta(y_2^- - y_1^-)\theta(y_3^-)] \quad (50)$$

is equivalent to the restrictions

$$|y_1^-|>|y_2^-|>|y_3^-|. \quad (51)$$

This means that the y_2^- and y_3^- integrals are limited by y_1^-, which gives no A enhancement because of the rapidly oscillating exponential $e^{ix_1p^+y_1^-}$. Since we are only concerned with terms including A enhancement, the first term in Eq. (49) can be ignored, leaving

$$\begin{aligned} T_{1-L}+T_{1-M}+T_{1-R} \simeq &-g^4\int \frac{dx_1}{t^2}\frac{(2\pi)^4}{2l^-}\delta\left[l^+ - \frac{l_\perp^2}{2l^-}\right]\frac{1}{(s+t+Q^2)}e^{ix_1p^+y_1^+} \\ &\times\left[\Gamma_{1-L}^{\mu\nu}\delta\left[x_1+\frac{u}{s+t+Q^2}\right]-\Gamma_{1-M}^{\mu\nu}\delta\left[x_1+\frac{\hat{u}}{s+t+Q^2}\right]\right]\theta(y_2^- - y_1^-)\theta(y_3^-), \end{aligned} \quad (52)$$

where $\hat{u}$ is given by Eq. (47d). Referring to the expression for $W^{\mu\nu}$ in Eq. (32), we recognize that these θ functions are exactly the conditions for final-state interactions.

If we fix $K_\perp=0$ before doing the contour integral, we get $\hat{u}=u$ and

$$\Gamma^{\mu\nu}_{1-M}(x_1P^+,x_2P^+,x_3P^+)=\Gamma^{\mu\nu}_{1-L}(x_1P^+,x_2P^+,x_3P^+)\,, \tag{53}$$

so that the second term in Eq. (49) also vanishes. This shows that the twist-two term in the collinear expansion [see Eqs. (17) and (21) in Sec. III]

$$\hat{H}^{\mu\alpha\beta\nu}(x_1P^+,x_2P^+,x_3P^+)\frac{P_\alpha P_\beta}{(P\cdot n)^2}\langle A|\bar{\psi}(y_1^-)n\cdot A(z_2)n\cdot A(z_3)\psi(0)|A\rangle$$

does not contribute to A enhancement. In fact, it reduces to an *eikonal* term for the twist-two distribution, $\langle A|\bar{\psi}(z_1)\psi(0)|A\rangle$ [19].

For a process in which the observed outgoing parton does not absorb soft gluons directly, we may expect no A enhancement even from its twist-four term like Eq. (32). An example at this order is shown in Fig. 4, where the soft gluons are absorbed by the "unobserved" final-state parton of momentum x_1P+q. Repeating the same procedure as above, for the three cut diagrams of Fig. 4 we find, in place of Eq. (49),

$$\begin{aligned}\int dx_1dx_2dx_3 \sum_{a=L,M,R}&\mathrm{Tr}[\hat{H}^{\mu\alpha\beta\nu}_a(x_1P^+,K_2,K_3)\not{P}P_\alpha P_\beta]e^{ix_1P^+y_1^-}e^{ix_2P^+y_2^-}e^{ix_3P^+y_3^-}\\
&=-g^4\int dx_1\frac{(2\pi)^4}{2l^-}\delta\left[l^+-\frac{l_\perp^2}{2l^-}\right]\frac{1}{(s+t+Q^2)^3}\delta\left[x_1+\frac{u}{s+t+Q^2}\right]\\
&\quad\times e^{ix_1P^+y_1^+}\exp\left[i\left[\frac{K_\perp^2-2K_\perp\cdot l_\perp}{s+t+Q^2}\right]P^+(y_2^--y_3^-)\right]\Gamma^{\mu\nu}_L\\
&\quad\times[\theta(y_2^--y_3^-)\theta(y_3^-)+\theta(y_3^--y_2^-)\theta(y_2^--y_1^-)-\theta(y_2^--y_1^-)\theta(y_3^-)]\,,\end{aligned} \tag{54}$$

which, by Eq. (51), does not contribute to A enhancement. We see that every cut diagram in Fig. 4 individually has at least one free integral, which may contribute to A enhancement, but when we sum over the three cut diagrams, the combination of the step functions produces a restriction that confines the integral to a small region compared to the nuclear size. Outside this small region, the integrals of the three cut diagrams cancel. Thus the cancellation in the sum over cuts eliminates A enhancement in this process. We may think of this as due to the cancellation of final-state interactions whenever the soft scatterings do not affect the momentum of the observed particle. On the other hand, in Fig. 3(M), $K_\perp$ flows through two poles and one final-state δ function. This leads to a relation between $K_\perp$ and x_1 which makes the result of Fig. 3(M) different from that of Figs. 3(L) and 3(R). In this case the final-state interactions affect the observed particle momentum directly, and Fig. 3 survives the cancellation between different cuts.

D. Summary of soft rescattering

In summary, the A enhancement in $W^{\mu\nu}$ from Fig. 3 turns out to be

$$\begin{aligned}W^{\mu\nu}=-\frac{g^4}{16}\int\frac{dy_1^-}{2\pi}\frac{dy_2^-}{2\pi}\frac{dy_3^-}{2\pi}&\mathrm{Tr}\{\langle A|\bar{\psi}(y_1^-)\not{n}F_{+\perp}(y_2^-)F_+{}^{\perp}(y_3^-)\psi(0)|A\rangle\}\\
&\times\nabla^2_{K_\perp}\left\{\int\frac{dx_1}{t^2}\frac{(2\pi)^4}{2l^-}\delta\left[l^+-\frac{l_\perp^2}{2l^-}\right]\frac{1}{(s+t+Q^2)}e^{ix_1P^+y_1^-}\right.\\
&\left.\left.\times\left[\Gamma^{\mu\nu}_{1-L}\delta\left[x_1+\frac{u}{s+t+Q^2}\right]-\Gamma^{\mu\nu}_{1-M}\delta\left[x_1+\frac{\hat{u}}{s+t+Q^2}\right]\right]\right\}\right|_{K_\perp=0}\theta(y_2^--y_1^-)\theta(y_3^-)\,,\end{aligned} \tag{55}$$

where

$$\nabla^2_{K_\perp}\equiv-\left.\frac{\partial^2}{\partial K_{2\perp}\partial K^{3\perp}}\right|_{K_{2\perp}=-K_{3\perp}\equiv K_\perp}\,. \tag{56}$$

If we define

$$M_q(x)\equiv\int\frac{dy_1^-}{2\pi}dy_2^-\frac{dy_3^-}{2\pi}e^{ix_1P^+y_1^-}\,\mathrm{Tr}\left[\langle A|\bar{\psi}(y_1^-)\frac{\not{n}}{2}F_{+\perp}(y_2^-)F_+{}^{\perp}(y_3^-)\psi(0)|A\rangle\right]\theta(y_2^--y_1^-)\theta(y_3^-)\,, \tag{57}$$

then

$$W^{\mu\nu}=-\frac{g^4}{16\pi}\frac{(2\pi)^4}{2l^-}\delta\left[l^+-\frac{l_\perp^2}{2l^-}\right]\frac{1}{t^2(s+t+Q^2)}\nabla^2_{K_\perp}[\Gamma^{\mu\nu}_{1-L}M_q(x)-\Gamma^{\mu\nu}_{1-M}M_q(\hat{x})]|_{K_\perp=0}\,, \tag{58}$$

where

$$x=-\frac{u}{s+t+Q^2}\ , \tag{59a}$$

$$\hat{x}=-\frac{\hat{u}}{s+t+Q^2}\ . \tag{59b}$$

Even though this expression is based on the example shown in Fig. 3, it is easy to check that it also applies to all of the diagrams in Fig. 2, so that we only need to calculate the $\Gamma^{\mu\nu}_{i-L}$ and $\Gamma^{\mu\nu}_{i-M}$ for each individual diagram with $i=1-8$.

Using current conservation $q_\mu \hat{H}^{\mu\alpha\beta\nu}=q_\nu \hat{H}^{\mu\alpha\beta\nu}=0$, the leptonic tensor [Eq. (14b)] $L_{\mu\nu}=\mathrm{Tr}\{\not{L}\gamma^\mu \not{L}'\gamma^\nu\}$, with $L'_\mu=L_\mu-q_\mu$, can be replaced by

$$L_{\mu\nu}=4\left[2L_\mu L_\nu-\frac{Q^2}{2}g_{\mu\nu}\right]\ , \tag{60}$$

where L_μ and L_ν are defined in Eqs. (12a)–(12d) (Sec. II). Combining Eqs. (58), (60), and (14a), we find

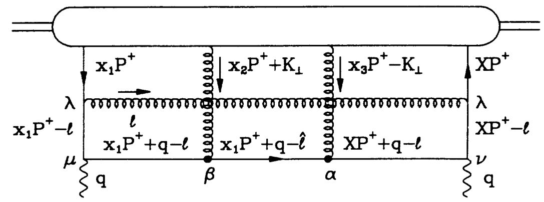

(L)

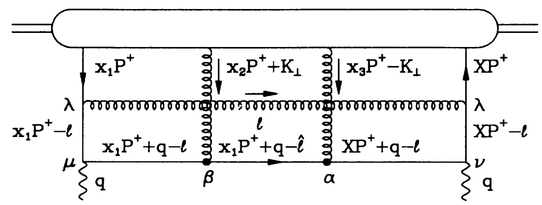

(M)

FIG. 4. Sample diagram for soft rescattering that does not contribute to anomalous nuclear enhancement, because the soft rescattering is not on the observed parton line. Here we define $X\equiv x_1+x_2+x_3$. As in Fig. 3, we suppress a cut on the right.

$$E_{L'}E_l\frac{d\sigma_{qg}}{dL'^3dl^3}=\frac{\alpha_{\rm EM}^2\alpha_s^2e_q^2}{wQ^4t^2(s+t+Q^2)}\sum_{i=1}^{8}\nabla^2_{K_\perp}\left\{2[F_{i-M}(\hat{u},\hat{v})M_q(\hat{x})-F_{i-L}(u,v)M_q(x)]\right.$$
$$\left.+\frac{Q^2}{2}[N_{i-M}(\hat{u})M_q(\hat{x})-N_{i-L}(u)M_q(x)]\right\}\Bigg|_{K_\perp=0}\ , \tag{61}$$

where we define

$$v\equiv 2(L\cdot l)\ ,\quad \hat{v}\equiv 2(L\cdot\hat{l})\ , \tag{62}$$

and where $\alpha_s\equiv g^2/4\pi$. The index i goes from 1 to 8 corresponding to the eight diagrams in Fig. 2, and

$$F_{i-a}(u,v)=L_\mu L_\nu \Gamma^{\mu\nu}_{i-a}\ , \tag{63a}$$

$$N_{i-a}(u)=-g_{\mu\nu}\Gamma^{\mu\nu}_{i-a}\ , \tag{63b}$$

with $a=L$ and M. The results for F_{i-L} and N_{i-L} are given in Table I. The expressions for F_{i-M} and N_{i-M} can also be simply read from Table I by replacing u and v with $\hat{u}$ and $\hat{v}$. Note that the F_{i-a} and N_{i-a} in Eq. (61) include an appropriate color factor, whose staightforward calculation [21] is omitted here, but which is given in Table I. These color factors are computed assuming that the pairs of quark and gluon fields in M_q individually form color singlets, since they can be widely separated in the nucleus.

E. Four-gluon case

A similar formulation applies to the four-gluon case, where the two soft gluons play the same roles as above, but two hard gluons replace the two hard quarks (or antiquarks),

$$E_{L'}E_l\frac{d\sigma_{gg}}{dL'^3dl^3}=\frac{\alpha_{\rm EM}^2\alpha_s^2e_q^2}{wQ^4t^2(s+t+Q^2)}\sum_{i=9}^{10}\nabla^2_{K_\perp}\left\{2\left[F_{i-M}(\hat{u},\hat{v})\frac{M_g(\hat{x})}{\hat{x}}-F_{i-L}(u,v)\frac{M_g(x)}{x}\right]\right.$$
$$\left.+\frac{Q^2}{2}\left[N_{i-M}(\hat{u})\frac{M_g(\hat{x})}{\hat{x}}-N_{i-L}(u)\frac{M_g(x)}{x}\right]\right\}\Bigg|_{K_\perp=0}\ , \tag{64}$$

where the relevant matrix element is

$$\frac{M_g(x)}{x}=\int\frac{P^+dy_1^-}{2\pi}dy_2^-\frac{dy_3^-}{2\pi}e^{x_1P^+y_1^-}\langle A|A^\perp(y_1^-)F_{+\perp}(y_2^-)F_+{}^\perp(y_3^-)A_\perp(0)|A\rangle\theta(y_2^--y_1^-)\theta(y_3^-) \tag{65a}$$

or, equivalently,

TABLE I. Subprocess cross sections for the hard-quark—soft-gluon case, where $\gamma \equiv Q^2+u+xt$. Note that every N_i and F_i should be multiplied by a color factor. They are $C_{F_i}=\frac{2}{9}$ for $i=1$–4 and $C_{F_i}=\frac{1}{2}$ for $i=5$–8.

Fig. 2 diagram No.	Terms	Results
(1)	N_1	$\frac{8t^2}{x}\frac{\gamma}{[-x(s+t+Q^2)]}$
	F_1	$\frac{-4t^2v}{u^2}[(s+t+Q^2)(v+Q^2)+wu]$
(2)	N_2	$\frac{8t^2}{x}\frac{Q^2t}{\gamma(s+t+Q^2)}$
	F_2	$\frac{2t^2}{u\gamma}\{xw[t(v+Q^2)+w(u+Q^2)]+v[v(s+Q^2)+Q^2(w-t)]\}$
(4)	N_4	$\frac{8t^2}{x}\frac{[-x(s+t+Q^2)]}{\gamma}$
	F_4	$\frac{4t^2w}{\gamma}(Q^2+v-xw)$
(5)	N_5	$\frac{8t^2}{x}\frac{\gamma}{xt}$
	F_5	$\frac{4vt}{u^2}(Q^2+v-xw)(s+t+Q^2)^2$
(6)	N_6	$\frac{8t^2}{x}\frac{Q^2(s+t+Q^2)}{\gamma t}$
	F_6	$\frac{2t}{x\gamma}\{2xw[t(v+Q^2)+wQ^2]+(v+Q^2)[-Q^2t+(s+Q^2)v+w(u-Q^2)]\}$
(8)	N_8	$\frac{8t^2}{x}\frac{xt}{\gamma}$
	F_8	$\frac{-4t^2wv}{\gamma}$

$$xM_g(x)=\int\frac{dy_1^-}{2\pi}\frac{dy_2^-}{P^+}\frac{dy_3^-}{2\pi}e^{ix_1P^+y_1^-}\times\langle A|F^{+\perp}(y_1^-)F_{+\perp}(y_2^-)F_+{}^{\perp}(y_3^-)F^+{}_{\perp}(0)|A\rangle\times\theta(y_2^--y_1^-)\theta(y_3^-)\,. \quad (65b)$$

The definitions of the F's and N's are as above, but the indices $i=9,10$ correspond to the last two diagrams in Fig. 2. The results and relevant color factors are listed in Table II.

V. DOUBLE HARD SCATTERING

In DIS, double hard scatterings are allowed by the kinematics at the same order as soft rescattering. The virtual photon has spacelike momentum $q^2<0$, and so it can

TABLE II. Subprocess cross section for the four-gluon case, where the color factors are $C_{F_i}=\frac{1}{2}$ for $i=9,10$.

Fig. 2 diagram no.	Terms	Results
(9)	N_9	$8t^2\frac{s+t+Q^2}{-t}$
	F_9	$4t^2w\frac{Q^2+v-xw}{t}$
(10)	N_{10}	$8t^2\frac{-t}{s+t+Q^2}$
	F_{10}	$4t^2w\frac{v}{s+t+Q^2}$

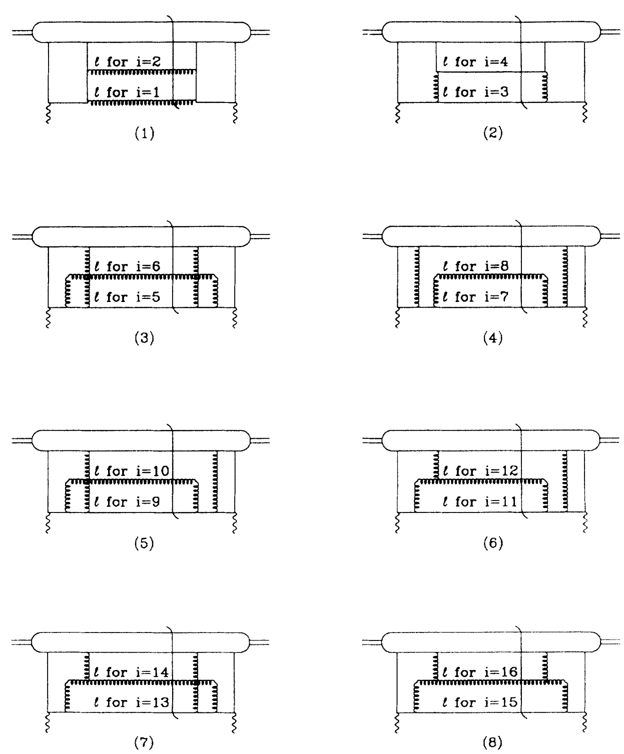

FIG. 5. Leading-order cut diagrams for double hard rescattering in lepton-hadron DIS. The parton of momentum l is observed in the final state. There are 8 diagrams and total of 16 ($i=1,2,\ldots,16$) possibilities for the observed parton.

be absorbed by an on-shell initial quark with large momentum $x_B P^+$ to form an on-shell intermediate quark, which may in turn be scattered by another nuclear parton, also with large longitudinal momentum $(x - x_B)P^+$ with x given by Eq. (59a).

The propagators of the intermediate on-shell quarks have poles in the corresponding Feynman diagrams, and these poles can eliminate phases and produce A enhancement in much the same way as for soft rescattering. The process is rather straightforward, and the physical mechanism is revealed directly in the cut diagrams, which are shown in Fig. 5.

Three notable properties in the calculations of double hard scatterings should be mentioned.

(i) The leading behavior of all of the double hard scatterings is twist-four.

(ii) For every individual double hard scattering contributing to A enhancement, the cut is only through the middle of the cut diagram, and so there is no need of cancellation between cuts. This makes the calculations much simpler than for the case of soft rescattering, discussed in Sec. III.

(iii) It is easy to see that the hard part of a double hard scattering, $\hat{H}_i^{\mu\nu}$, is always of a common form

$$\hat{H}_i^{\mu\nu} = \mathrm{Tr}[\not{P}\gamma^\mu(x_B\not{P}+\not{q})\hat{K}_i(x_B\not{P}+\not{q})\gamma^\nu] \ , \tag{66}$$

where the matrix $\hat{K}_i$ depends on each individual subprocess with index $i = 1-16$ illustrated in Fig. 5. (There are eight diagrams in Fig. 5, but each diagram gives two contributions, depending on which particle is observed.) We see that the $\hat{K}_i$ is always placed between two on-shell lines carrying the same momentum $x_B P^+ + q$, which gives us the benefit that, even without knowing the specific form of $\hat{K}_i$, we have, for any double hard scattering process,

$$\left[2L_\mu L_\nu - \frac{Q^2}{2} g_{\mu\nu}\right]\hat{H}_i^{\mu\nu} = Q^2 \left[X^2 - X + \frac{1}{2}\right] N_i \ , \tag{67}$$

with, as in Eq. (63b), $N_i \equiv -g_{\mu\nu}\hat{H}_i^{\mu\nu}$ and $X \equiv w/(s+Q^2)$, where w is defined in Eq. (13).

The double hard scatterings occur for both four-quark cases and two-gluon + two-quark cases. The four-quark double hard scatterings include four sorts of processes shown in Fig. 5, diagrams (1) and (2), respectively. For Fig. 5, diagram (1), we have

$$E_{L'}E_l \frac{d\tilde{\sigma}_1^{qq}}{dL'^3 dl^3} = \frac{2\alpha_{\mathrm{EM}}^2\alpha_s^2 e_q^2}{wQ^2(s+Q^2)^2(s+t+Q^2)}\left[X^2 - X + \frac{1}{2}\right]\sum_i \tilde{N}_i^{qq}\tilde{M}_I^{qq}(x) \ , \tag{68}$$

with $i = 1$ and 2, where the relevant matrix elements are

$$\begin{aligned}\tilde{M}_I^{qq}(x) \equiv \int \frac{dy_1^-}{2\pi}P^+ dy_2^- \frac{dy_3^-}{2\pi} e^{ix_BP^+y_1^-} e^{i(x-x_B)P^+(y_2^- - y_3^-)} \\ \times \left\{\left\langle A\left|\mathrm{Tr}\left[\frac{\not{n}}{2}\psi(y_1^-)\bar{\psi}(0)\right]\left[\bar{\psi}(y_2^-)\frac{\not{n}}{2}\psi(y_3^-)\right]\right|A\right\rangle\right. \\ \left. + \left\langle A\left|\left[\bar{\psi}(y_1^-)\frac{\not{n}}{2}\psi(0)\right]\mathrm{Tr}\left[\frac{\not{n}}{2}\psi(y_2^-)\bar{\psi}(y_3^-)\right]\right|A\right\rangle\right\}\theta(y_2^- - y_1^-)\theta(y_3^-) \ .\end{aligned} \tag{69}$$

Here and below, we use a tilde on the σ's, N's, and M's to identify double hard scattering. The two matrix elements correspond to scattering from quarks and/or antiquarks at different locations in the nucleus. The Tr proceeding the $\not{n}\psi\bar{\psi}$ combination indicates that there are no free Dirac indices. A summation over the indices of $\bar{\psi}\not{n}\psi$ combinations is understood.

Similarly, for Fig. 5, diagram (2), we have

$$E_{L'}E_l \frac{d\tilde{\sigma}_2^{qq}}{dL'^3 dl^3} = \frac{2\alpha_{\mathrm{EM}}^2\alpha_s^2 e_q^2}{wQ^2(s+Q^2)^2(s+t+Q^2)}\left[X^2 - X + \frac{1}{2}\right]\tilde{N}_i^{qq}\tilde{M}_{II}^{qq}(x) \ , \tag{70}$$

with $i = 3$ and 4, and

$$\begin{aligned}\tilde{M}_{II}^{qq}(x) \equiv \int \frac{dy_1^-}{2\pi}P^+ dy_2^- \frac{dy_3^-}{2\pi} e^{ix_BP^+y_1^-} e^{i(x-x_B)P^+(y_2^- - y_3^-)} \\ \times \left\{\left\langle A\left|\mathrm{Tr}\left[\frac{\not{n}}{2}\psi(y_1^-)\bar{\psi}(0)\right]\mathrm{Tr}\left[\frac{\not{n}}{2}\psi(y_2^-)\bar{\psi}(y_3^-)\right]\right|A\right\rangle\right. \\ + \left\langle A\left|\mathrm{Tr}\left[\frac{\not{n}}{2}\psi(y_1^-)\bar{\psi}(0)\right]\left[\bar{\psi}(y_2^-)\frac{\not{n}}{2}\psi(y_3^-)\right]\right|A\right\rangle \\ + \left\langle A\left|\left[\bar{\psi}(y_1^-)\frac{\not{n}}{2}\psi(0)\right]\mathrm{Tr}\left[\frac{\not{n}}{2}\psi(y_2^-)\bar{\psi}(y_3^-)\right]\right|A\right\rangle \\ \left. + \left\langle A\left|\left[\bar{\psi}(y_1^-)\frac{\not{n}}{2}\psi(0)\right]\left[\bar{\psi}(y_2^-)\frac{\not{n}}{2}\psi(y_3^-)\right]\right|A\right\rangle\right\}\theta(y_2^- - y_1^-)\theta(y_3^-) \ .\end{aligned} \tag{71}$$

The other kind of double hard scattering at lowest order has two nuclear quarks and two gluons in its cut diagram. It includes 12 individual processes shown in Fig. 5, diagrams (3)–(8). The cross section is

$$E_{L'}E_l\frac{d\tilde{\sigma}_i{}^{qg}}{dL'^3dl^3}=\frac{2\alpha_{\rm EM}^2\alpha_s^2e_q^2}{wQ^2(s+Q^2)^2(s+t+Q^2)}\left[X^2-X+\frac{1}{2}\right]\tilde{N}_i{}^{qg}\tilde{M}^{qg}(x)\ , \tag{72}$$

with $i=1-12$, and

$$\tilde{M}^{qg}(x)\equiv\int\frac{dy_1^-}{2\pi}P^+dy_2^-\frac{P^+dy_3^-}{2\pi}e^{ix_BP^+y_1^-}e^{i(x-x_B)P^+(y_2^--y_3^-)}$$
$$\times\left\{\left\langle A\left|\mathrm{Tr}\left[\frac{\not{n}}{2}\psi(y_1^-)A_\perp(y_2^-)A^\perp(y_3^-)\bar{\psi}(0)\right]\right|A\right\rangle\right.$$
$$\left.+\left\langle A\left|\left[\bar{\psi}(y_1^-)\frac{\not{n}}{2}A_\perp(y_2^-)A^\perp(y_3^-)\psi(0)\right]\right|A\right\rangle\right\}\theta(y_2^--y_1^-)\theta(y_3^-)\ . \tag{73}$$

The results for $\tilde{N}_i{}^{qq}$ $(i=1-4)$ and $\tilde{N}_i{}^{qg}$ $(i=1-12)$ and their color factors are given in Table III. At lowest order, double hard scattering cannot occur with four gluon fields.

VI. A DEPENDENCE AND MATRIX ELEMENTS

We have argued above that matrix elements such as $M_q(x)$ [Eq. (57)] grow as $A^{4/3}$. In this section, we will explore this claim, basing it on ideas of color confinement and approximate translational invariance within the nucleus. We also briefly discuss the relative sizes of matrix elements involving transverse and longitudinal components of the gluon field and justify our assertion, made after Eq. (21), that in soft rescatterings the fields $\omega_\alpha{}^{\alpha'}A_{\alpha'}$ may be neglected compared to $n\cdot A$ (in covariant gauges).

All the twist-four matrix elements identified above include two pairs of field operators, for example,

TABLE III. Subprocess cross section for double scattering, where $\gamma\equiv Q^2+u+xt$.

Fig. 6 diagram No.	Terms	C_{F_i}	Results
(1)	$\tilde{N}_1^{qq}$	$\frac{1}{12}$	$\frac{16t(s+Q^2)^2}{(s+t+Q^2)\gamma}$
	$\tilde{N}_2^{qq}$	$\frac{1}{12}$	$\frac{16(s+t+Q^2)(s+Q^2)^2}{t\gamma}$
(2)	$\tilde{N}_3^{qq}$	$\frac{1}{32}$	$\frac{-16(s+Q^2)^2[(s+Q^2)^2+t^2]}{(s+t+Q^2)^2\gamma}$
	$\tilde{N}_4^{qq}$	$\frac{1}{32}$	$\frac{-16(s+Q^2)^2[(s+Q^2)^2+(s+t+Q^2)^2]}{t^2\gamma}$
(3)	$\tilde{N}_1^{qg}$	$\frac{2}{9}$	$\frac{16(s+Q^2)^2}{-t}$
	$\tilde{N}_2^{qg}$	$\frac{2}{9}$	$\frac{16(s+Q^2)^2}{s+t+Q^2}$
(4)	$\tilde{N}_3^{qg}$	$\frac{2}{9}$	$-16t$
	$\tilde{N}_4^{qg}$	$\frac{2}{9}$	$16(s+t+Q^2)$
(5)	$\tilde{N}_5^{qg}$		0
	$\tilde{N}_6^{qg}$		0
(6)	$\tilde{N}_7^{qg}$	$\frac{1}{4}$	$2\frac{(-16)(s+Q^2)^2}{s+t+Q^2}$
	$\tilde{N}_8^{qg}$	$\frac{1}{4}$	$2\frac{16(s+Q^2)^2}{t}$
(7)	$\tilde{N}_9^{qg}$	$-\frac{1}{4}$	$2\frac{16(s+Q^2)t}{s+t+Q^2}$
	$\tilde{N}_{10}^{qg}$	$-\frac{1}{4}$	$2\frac{16(s+Q^2)(s+t+Q^2)}{t}$
(8)	$\tilde{N}_{11}^{qg}$	$\frac{1}{2}$	$\frac{8[-5t(s+Q^2)+4(s+t+Q^2)^2](s+Q^2)}{(s+t+Q^2)^2}$
	$\tilde{N}_{12}^{qg}$	$\frac{1}{2}$	$\frac{8[5(s+t+Q^2)(s+Q^2)+4t^2](s+Q^2)}{t^2}$

$F_{+\perp}(y_2^-)F_+{}^{\perp}(y_3^-)$ and $\bar{\psi}(y_1^-)\psi(0)$ in $M_q(x)$ [Eq. (57)]. Given confinement, we believe that there are no long-distance color correlations in a nucleus. Therefore, in the matrix elements consisting of these field operators, we require

$$|y_2^- - y_3^-| \ll R_A , \tag{74}$$

$$|y_1^-| \ll R_A , \tag{75}$$

where R_A is the nuclear radius. Without these restrictions, at least two free integrals would remain in the $W^{\mu\nu}$s, for example, Eq. (55), suggesting that the cross section would grow as $A^{5/3}$ instead of $A^{4/3}$. The pair of operators $F_{+\perp}(y_2^-)F_+{}^{\perp}(y_3^-)$, however, are a Lorentz scalar and color singlet, and so we may expect that its expectation at fixed $y_2^- - y_3^- \ll R_A$ is relatively independent of y_3^-. Then the remaining free integral $\int dy_3^-$ should be of order $A^{1/3}$. In addition, to be consistent with the parton model, we may suggest that for fixed y_3 the nuclear matrix element

$$\int dy_1^- e^{ix_1P^+y_1^-} \langle A|\bar{\psi}(y_1^-)F_{+\perp}(y_2^-)F_+{}^{\perp}(y_3^-)\psi(0)|A\rangle \tag{76}$$

grows linearly with A. Of course, the proportionality is approximate and does not exclude all deviations from exact linearity, but only those deviations that grow with A. We justify this claim in terms of the following discussion.

Let $\hat{O}(Z)$ be a local operator at point Z or a pair of operators integrated over a region around Z that does not grow with the nuclear radius. Relevant examples of the latter case are, for us, $\int dy_2^- F_{+\perp}(y_2^-)F_+{}^{\perp}(y_3^-)$ and $\int dy_1^- e^{ix_1P^+y_1^-}\bar{\psi}(y_1^-)\psi(0)$. As indicated above, the latter pair of operators is restricted to a small region by oscillations of the phase $e^{ix_1P^+y_1^-}$ and the former by color confinement. Now let us consider the matrix element of $\hat{O}$ between nuclear coordinate eigenstates $\langle \mathbf{X}|$ and $|\mathbf{X}'\rangle$. The following assumption embodies the idea of approximate translation invariance in a large nucleus:

$$\langle \mathbf{X}|\hat{O}(z)|\mathbf{X}'\rangle = C_O\langle \mathbf{X}|\mathbf{X}'\rangle\theta(R_A - |\mathbf{X}-\mathbf{Z}|) , \tag{77}$$

where C_O is an arbitrary constant, independent of Z, $\mathbf{X}$ and $\mathbf{X}'$. That is, we assume that the expectation value of $\hat{O}(Z)$ is a constant if the point Z is inside the nucleus and zero if it is outside. In addition, the action of the almost-local operator $\hat{O}$ does not "move" the nucleus as a whole. Naturally, corrections to (77) are important, but we do not expect them to grow with A.

We normalize the nuclear state independently of A by

$$\langle \mathbf{P}_A|\mathbf{P}'_A\rangle = \frac{2\omega_A}{A}\delta^3(\mathbf{P}_A - \mathbf{P}'_A) \tag{78}$$

or, equivalently,

$$\langle \mathbf{P}_A|\mathbf{X}\rangle = \frac{\sqrt{2\omega_A/A}}{(2\pi)^{3/2}}e^{i\mathbf{P}_A\cdot\mathbf{X}} , \tag{79}$$

where $\mathbf{P}_A$ and ω_A are the momentum and the energy of the nucleus. As we will now show, the assumption Eq. (77) combined with the normalization Eq. (79) leads to $\langle \mathbf{P}_A|\hat{O}_1\hat{O}_2|\mathbf{P}'_A\rangle \propto A$, with $\hat{O}_1$ and $\hat{O}_2$ operators of the type just discussed above.

Now let us expand our typical four-field expectation value in terms of a complete set of states,

$$\langle \mathbf{P}_A|\hat{O}_1(y)\hat{O}_2(0)|\mathbf{P}_A\rangle = \int d^3X_1d^3X_2d^3X_3\langle \mathbf{P}_A|\mathbf{X}_1\rangle\langle \mathbf{X}_1|\hat{O}_1(y)|\mathbf{X}_2\rangle\langle \mathbf{X}_2|\hat{O}_2(0)|\mathbf{X}_3\rangle\langle \mathbf{X}_3|\mathbf{P}'_A\rangle + \dots , \tag{80}$$

where the terms that are suppressed involve excited states of the nucleus, not expressible in terms of the coordinate eigenstates $|\mathbf{X}\rangle$. Then, applying the assumption Eq. (77) to $\hat{O}_1$ and $\hat{O}_2$, we get

$$\langle \mathbf{P}_A|\hat{O}_1\hat{O}_2|\mathbf{P}_A\rangle = C_{O_1}C_{O_2}\int d^3X_1d^3X_2d^3X_3\langle \mathbf{P}_A|\mathbf{X}_1\rangle\langle \mathbf{X}_1|\mathbf{X}_2\rangle\langle \mathbf{X}_2|\mathbf{X}_3\rangle\langle \mathbf{X}_3|\mathbf{P}'_A\rangle\theta(R_A - |\mathbf{X}_1 - y|)\theta(R_A - |\mathbf{X}_2|) , \tag{81}$$

where again we suppress the contributions of excited states. By the normalization Eq. (79) and $\langle \mathbf{X}_1|\mathbf{X}_2\rangle = \delta^3(\mathbf{X}_1 - \mathbf{X}_2)$, we have

$$\langle \mathbf{P}_A|\hat{O}_1\hat{O}_2|\mathbf{P}_A\rangle = C_{O_1}C_{O_2}\frac{\sqrt{4\omega_A\omega'_A}}{A(2\pi)^3}\int d^3X_1\theta(R_A - |\mathbf{X}_1 - \mathbf{y}|)\theta(R_A - |\mathbf{X}_2|) . \tag{82}$$

As long as $|\mathbf{y}| < 2R_A$, this scales as the nuclear volume and hence as A. Equally, important, the expectation is independent of the distance between the operators, and the dependence on the operators factorizes into the constants $C_{O_1}C_{O_2}$.

The consequences of this reasoning for matrix elements such as $M_q(x)$ are now straightforward. If, for instance, we have chosen $O_1 = I$, the identity operator above, with $O_2 = \int dy_1^- e^{ix_1P^+y_1^-}\bar{\psi}(y_1^-)\psi(0)$, we would conclude that C_2 was proportional to the quark parton distribution in the nucleus. The effect of inserting the soft-gluon combination $\int dy_2^- F_{+\perp}(y_2^-)F_+{}^{\perp}(y_3^-)$, at fixed y_3^-, however, is summarized simply by a multiplicative factor. Then, for $y = y_3$ in the minus direction, the integral over y^- in Eq. (82) reduces precisely to the geometrical estimates of double scattering found, for instance, in the papers of Ref. [13] and gives an extra overall factor $A^{1/3}$, again times overall constants.

In summary, the matrix element $M_q(x)$ differs from the quark distribution $q(x)$ in the same nucleus by an overall factor, which we denote λ^2 below. Indeed, this factor should be the same whether the hard parton is a quark, as in $M_q(x)$ [Eq. (57)], or a gluon, as in $M_q(x)$ [Eq. (65a)]. Thus we take as phenomenological expressions for the twist-four matrix elements that occur in soft rescattering the following [16,21]:

$$M_q(x)=A^{4/3}\lambda^2 q(x)\ , \tag{83}$$

$$\frac{M_q(x)}{x}=A^{4/3}\lambda^2\frac{G(x)}{x}\ . \tag{84}$$

Here λ^2 has units of mass squared. In Ref. [21] we showed that the dijet momentum imbalance in photoproduction [9] is consistent with λ^2 in the range 0.05–0.1 GeV^2.

For the twist-four matrix elements that occur in double hard scattering [Sec. V, Eqs. (69), (71), and (73)], we adopt the model of Ref. [24] and take

$$\tilde{M}_I^{qq}(x_B,x-x_B)=CA^{4/3}q(x_B)\bar{q}(x-x_B)\ , \tag{85a}$$

$$\tilde{M}_{II}^{qq}(x_B,x-x_B)=CA^{4/3}q(x_B)q(x-x_B)\ , \tag{85b}$$

$$\tilde{M}^{qg}(x_B,x-x_B)=CA^{4/3}q(x_B)\frac{G(x-x_B)}{x-x_B}\ , \tag{85c}$$

where $q(x)$ is a normal twist-two quark (or antiquark) distribution, $G(x)$ is a corresponding gluon distribution, and C is constant in GeV^2, $C=(0.35/8\pi\chi^2)\ \mathrm{GeV}^2$, with $\chi\approx1.1-1.25$.

In Sec. III we needed to compare the integrals $(A^+=n\cdot A)$,

$$\int dy_i^-\,A^+(y_i^-)\ \text{ and }\ \int dy_i^-\,\omega_\alpha{}^{\alpha'}A_{\alpha'}(y_i^-)\ , \tag{86}$$

inserted in matrix elements, to identify terms that contribute to A enhancement in the collinear expansion of Eq. (21). We claimed that in a covariant gauge the first is larger than the second by a power of P^+ in the center-of-mass frame of Sec. II. In the following, we justify this claim.

We note first that the first integral $\int dy_i^-\,A^+(y_i^-)$ in Eq. (86) is boost invariant in a covariant gauge, while the other is not. To compare them we rewrite the second integral as

$$\int dy_i^-\,\omega_\alpha{}^{\alpha'}A_{\alpha'}(y_i^-)=\frac{1}{P^+}\int dy_i^-\,P^+\omega_\alpha{}^{\alpha'}A_{\alpha'}(y_i^-)\ . \tag{87}$$

Now the right side of Eq. (87), apart from a factor of $1/P^+$, is boost invariant. The two boost-invariant integrals

$$\int dy_i^-\,A^+(y_i^-)\ \text{ and }\ \int dy_i^-\,P^+\omega_\alpha{}^{\alpha'}A_{\alpha'}(y_i^-)$$

have magnitudes set by nucleon and nuclear scales. Now, however, the integral $\int dy_i^-\,\omega_\alpha{}^{\alpha'}A^{\alpha'}(y_i^-)$ appears with an explicit additional factor $1/P^+$, which will have to combine to form a large invariant $1/t\sim1/u\sim\ldots$ in the cross section. Thus, terms associated with $\omega_\alpha{}^{\alpha'}A^+(y_i^-)$ are suppressed by a power of the large momentum transfer compared with $n\cdot A$ terms in covariant gauge.

VII. PHOTOPRODUCTION

In photoproduction, the incident photon is real, and so $q_\mu q^\mu=0$. As a result, we cannot use the kinematics of Sec. II. The relevant Mandelstam variables are now

$$s\equiv(p+q)^2=2P^+q^-\ , \tag{88}$$

$$u\equiv(l-q)^2=-2l^+q^-\ , \tag{89}$$

while t is unchanged compared to Eq. (38b).

At the order we consider, A enhancement in photoproduction comes entirely from additional soft scatterings; double hard scattering does not contribute to the nuclear dependence in photoproduction.

The procedure for computing the single-jet cross section $d\sigma/d^3l$ in spin-averaged photoproduction is essentially identical to that for DIS. The resulting lowest-order cross sections have been given in Ref. [16]. They can also be derived directly from the DIS results [Eq. (64)] in the following manner.

Consider the definitions of F_i and N_i in Eqs. (63a) and (63b) and of the leptonic tensor $L_{\mu\nu}$ [Eq. (60)]. To derive the photoproduction single-jet cross section from the DIS cross section, we need to (i) replace the lepton tensor $L_{\mu\nu}$ by a sum over photon polarizations, $-g_{\mu\nu}$, and hence [see Eqs (60)–(63b)] drop all F_i terms and divide N_i terms by $e^2Q^2/2$; (ii) multiply by $Q^4(2\pi)^3$ to eliminate the extra factors associated with the exchanged photon and the phase space of the outgoing lepton in DIS; and (iii) replace w [Eq. (13)] by $s=(q+p)^2$. The result of this procedure is the cross section given in Ref. [16]:

$$E_l\frac{d\sigma_{qg}}{dl^3}=\frac{\alpha_{\mathrm{EM}}(\pi\alpha_s)^2H_q}{st^2(s+t)}\nabla^2_{K_\perp}\left[\frac{M_q(\hat{x})}{\hat{x}}-\frac{M_q(x)}{x}\right]\Bigg|_{K_\perp=0} \tag{90}$$

for the hard-quark—soft-gluon case and

$$E_l\frac{d\sigma_{gg}}{dl^3}=\frac{\alpha_{\mathrm{EM}}(\pi\alpha_s)^2H_g}{st^2(s+t)}\nabla^2_{K_\perp}\left[\frac{M_g(\hat{x})}{\hat{x}}-\frac{M_g(x)}{x}\right]\Bigg|_{K_\perp=0} \tag{91}$$

for the hard-gluon–soft-gluon case, where

$$H_q=4t^2\left[\frac{N^2-1}{2N^2}\left[\frac{s}{s+t}+\frac{s+t}{s}\right]+\left[\frac{s}{-t}+\frac{-t}{s}\right]\right] \tag{92}$$

and

$$H_g=4t^2\frac{1}{2N}\left[\frac{-t}{s+t}+\frac{s+t}{-t}\right]\ , \tag{93}$$

with $N=3$ the number of colors. Here color factors are included in Eqs. (92) and (93).

VIII. NUMERICAL RESULTS

A. Preparing for computation

For convenience of numerical computation, we reexpress the derivative $\nabla^2_{K_\perp}$ in Eqs. (61) and (64) in terms of invariants. To do this we expand, for example, $N_i(\hat{u})M_q(\hat{x})$ and $F_i(\hat{u},\hat{v})M_q(\hat{x})$ in Eq. (61) in terms of $(\hat{u}-u)$ and $(\hat{v}-v)$. Recall that u and v are defined in Eqs. (38c) and (62), respectively, and that x is specified for soft rescattering by Eq. (59a). This procedure gives

$$N_i(\hat{u},\hat{v})M_q(\hat{x})\approx N_i(u)M_q(x)+(\hat{u}-u)\left[\frac{\partial N_i(u)}{\partial u}M_q(x)-\frac{1}{s+t+Q^2}N_i(u)\frac{\partial M_q(x)}{\partial x}\right]$$
$$+\frac{1}{2}(\hat{u}-u)^2\left[\frac{\partial^2 N_i(u)}{\partial u^2}M_q(x)-\frac{2}{s+t+Q^2}\frac{\partial N_i(u)}{\partial u}\frac{\partial M_q(x)}{\partial x}+\frac{1}{(s+t+Q^2)^2}N_i(u)\frac{\partial^2 M_q(x)}{\partial x^2}\right], \quad (94)$$

$$F_i(\hat{u},\hat{v})M_q(\hat{x})\approx F_i(u)M_q(x)+(\hat{u}-u)\left[\frac{\partial F_i(u,v)}{\partial u}M_q(x)-\frac{1}{s+t+Q^2}F_i(u,v)\frac{\partial M_q(x)}{\partial x}\right]$$
$$+\frac{1}{2}(\hat{u}-u)^2\left[\frac{\partial^2 F_i(u,v)}{\partial u^2}M_q(x)-\frac{2}{s+t+Q^2}\frac{\partial F_i(u,v)}{\partial u}\frac{\partial M_q(x)}{\partial x}\right.$$
$$\left.+\frac{1}{(s+t+Q^2)^2}F_i(u,v)\frac{\partial^2 M_q(x)}{\partial x^2}\right]+(\hat{v}-v)\frac{\partial F_i(u,v)}{\partial v}M_q(x)+\frac{1}{2}(\hat{v}-v)^2\frac{\partial^2 F_i(u,v)}{\partial v^2}M_q(x)$$
$$+\frac{1}{2}(\hat{u}-u)(\hat{v}-v)\left[\frac{\partial^2 F_i(u,v)}{\partial u\,\partial v}M_q(x)-\frac{1}{s+t+Q^2}\frac{\partial F_i(u,v)}{\partial v}\frac{\partial M_q(x)}{\partial x}\right]. \quad (95)$$

In addition, we need the identities

$$\nabla^2_{K_\perp}(\hat{u}-u)=4\frac{Q^2}{x_B t}, \quad (96a)$$

$$\nabla^2_{K_\perp}[(\hat{u}-u)^2]=8\left[\frac{Q^2}{x_B t}\right]^2 l_\perp^2, \quad (96b)$$

$$\nabla^2_{K_\perp}(\hat{v}-v)=-4\frac{w}{t}, \quad (96c)$$

$$\nabla^2_{K_\perp}[(\hat{v}-v)^2]=8\left[\frac{w}{t}l_\perp+L_\perp\right]^2, \quad (96d)$$

$$\nabla^2_{K_\perp}[(\hat{u}-u)(\hat{v}-v)]=-8\frac{Q^2}{x_B t}\left[\frac{w}{t}l_\perp{}^2+l_\perp\cdot L_\perp\right]. \quad (96e)$$

Combining Eqs. (94) and (96a)–(96e) with Eq. (61), we have for the hard-quark–soft-gluon case in DIS,

$$E_{L'}E_l\frac{d\sigma_{qg}}{dL'^3dl^3}=\frac{\alpha^2_{\rm EM}\alpha_s^2}{wQ^4t^2(s+t+Q^2)}\left\{2Q^2\left\{\frac{Q^2}{x_B t}\left[\frac{\partial N_i(u)}{\partial u}M_q(x)-\frac{1}{s+t+Q^2}N_i(u)\frac{\partial M_q(x)}{\partial x}\right]\right.\right.$$
$$+\left[\frac{Q^2}{x_B t}\right]^2 l_\perp^2\left[\frac{\partial^2 N_i(u)}{\partial u^2}M_q(x)-\frac{2}{s+t+Q^2}\frac{\partial N_i(u)}{\partial u}\frac{\partial M_q(x)}{\partial x}\right.$$
$$\left.\left.+\frac{1}{(s+t+Q^2)^2}N_i(u)\frac{\partial^2 M_q(x)}{\partial x^2}\right]\right\}$$
$$+8\left\{\frac{Q^2}{x_B t}\left[\frac{\partial F_i(u,v)}{\partial u}M_q(x)-\frac{1}{s+t+Q^2}F_i(u,v)\frac{\partial M_q(x)}{\partial x}\right]\right.$$
$$+\left[\frac{Q^2}{x_B t}\right]^2 l_\perp^2\left[\frac{\partial^2 F_i(u,v)}{\partial u^2}M_q(x)-\frac{2}{s+t+Q^2}\frac{\partial F_i(u,v)}{\partial u}\frac{\partial M_q(x)}{\partial x}\right.$$

$$+\frac{1}{(s+t+Q^2)^2}F_i(u,v)\frac{\partial^2 M_q(x)}{\partial x^2}\Bigg]$$
$$-\frac{w}{t}\frac{\partial F_i(u,v)}{\partial v}M_q(x)+\left[\frac{w}{t}l_\perp+L_\perp\right]^2\frac{\partial^2 F_i(u,v)}{\partial v^2}M_q(x)$$
$$-\frac{Q^2}{x_B t}\left[\frac{w}{t}l_\perp^2+l_\perp\cdot L_\perp\right]\left[\frac{\partial^2 F_i(u,v)}{\partial u\,\partial v}M_q(x)-\frac{1}{s+t+Q^2}\frac{\partial F_i(u,v)}{\partial v}\frac{\partial M_q(x)}{\partial x}\right]\Bigg\}\Bigg] . \quad (97)$$

In this expression we will use the (hard-quark–soft-gluon) twist-four distribution function [Eq. (83)]

$$M_q(x)=A^{4/3}\lambda^2\sum_f e_{q_f}^2 q_f(x) , \quad (98)$$

where e_{q_f} is the electric charge of a quark with flavor $f=u,d,s,\ldots$ in units of electron charge. As mentioned above, λ^2 has been estimated in Ref. [21] to be of order 0.05–0.1 GeV^2.

Similarly for the four-gluon case in DIS, we find

$$E_{L'}E_l\frac{d\sigma_{gg}}{dL'^3dl^3}=\frac{\alpha_{\rm EM}^2\alpha_s^2}{wQ^4t^2(s+t+Q^2)}\left[\sum_f e_{q_f}^2\right]$$
$$\times\Bigg[2Q^2N_i\left[-\frac{Q^2}{x_Bt(s+t+Q^2)}\frac{\partial[M_g(x)/x]}{\partial x}+\left[\frac{Q^2}{x_Bt}\right]^2\frac{l_\perp^2}{(s+t+Q^2)^2}\frac{\partial^2[M_g(x)/x]}{\partial x^2}\right]$$
$$+8\Bigg\{F_i(v)\left[-\frac{Q^2}{x_Bt(s+t+Q^2)}\frac{\partial[M_g(x)/x]}{\partial x}+\left[\frac{Q^2}{x_Bt}\right]^2\frac{l_\perp^2}{(s+t+Q^2)^2}\frac{\partial^2[M_g(x)/x]}{\partial x^2}\right]$$
$$-\frac{w}{t}\frac{\partial F_i(v)}{\partial v}\frac{M_g(x)}{x}+\frac{Q^2}{x_Bt}\frac{(w/t)l_\perp^2+l_\perp\cdot L_\perp}{s+t+Q^2}\frac{\partial F_i(v)}{\partial v}\frac{\partial[M_g(x)/x]}{\partial x}\Bigg\}\Bigg] . \quad (99)$$

From Table III, we note that in the four-gluon case the $N_i\equiv N_{i-L}$ are functions of s, t, and Q^2 only, while the $F_i\equiv F_{i-L}$ are functions of s, t, Q^2, w, and v. Both the F_i and the N_i are independent of u.

Reducing to photoproduction, we have

$$E_l\frac{d\sigma}{dl^3}=\frac{2\alpha_{\rm EM}(\pi\alpha_s)^2}{st^2(s+t)}\left\{\sum_f[e_{q_f}^2\Phi_{q_f}(x,A)]H_q+\left[\sum_f e_{q_f}^2\right]\Phi_g(x,A)H_g\right\} , \quad (100)$$

where

$$\Phi_i(x,A)=\frac{s}{-t(s+t)}\frac{\partial[M_i(x)/x]}{\partial x}+\left[\frac{s}{-t(s+t)}\right]^2 l_\perp^2\frac{\partial^2[M_i(x)/x]}{\partial x^2} , \quad (101)$$

with $i=q_f$ and g corresponding to hard-quark–soft-gluon and four-gluon cases, respectively. The H_q and H_g have been given by Eqs. (92) and (93) in Sec. VII.

The expressions for double hard scattering, given above in Eqs. (68)–(73), are straightforward to evaluate numerically, using distributions with multiple quark flavors, generalizing Eqs. (85a)–(85c),

$$\tilde{M}_I^{qq}=CA^{4/3}\sum_f[e_{q_f}^2q_f(x_B)\bar{q}_f(x-x_B)] , \quad (102a)$$

$$\tilde{M}_{II}^{qq}=CA^{4/3}\sum_{q'}\left\{\sum_f[e_{q_f}^2q_f(x_B)]q_{f'}(x_B)\right\} , \quad (102b)$$

$$\tilde{M}^{qg}=CA^{4/3}\left[\sum_f e_{q_f}^2q_f(x_B)\right]\frac{G(x-x_B)}{x-x_B} . \quad (102c)$$

B. Phenomenological estimates

For the purposes of numerical evaluation, we simply choose the scaling parton distributions for $q_f(x)$ and $G(x)$, which are specified in Ref. [25]. The isospin ratio of the nuclear target is assumed as $Z/A=0.4$.

Numerical estimates have been given for photoproduction cross sections in Ref. [16] (with the estimate $\lambda^2=0.04$ GeV^2). Here we shall present results for high-p_T jets in DIS. The representative kinematic dependence of parameter $\alpha-1$, is computed from the definition

$$A\frac{d\sigma_1(A)}{d^3l}+\frac{d\sigma_{4/3}(A)}{d^3l}\equiv A^\alpha\frac{d\sigma_1(A)}{d^3l} , \quad (103)$$

where we take $A=200$ and where σ_1 is the leading-power nucleon Born cross section.

The leading power processes include ten diagrams similar to those of the additional soft scattering processes. These diagrams may be found from Fig. 2 by simply ignoring the extra soft gluons. Their cross sections for DIS take the form

$$E_{L'}E_l\frac{d\sigma}{dL'^3dl^3}=\sum_{i=1}^{10}\frac{\alpha_{\rm EM}^2\alpha_s}{(2\pi)^2wQ^4(s+t+Q^2)}\times[4F_i^0+Q^2N_i^0]M_i(x)\ , \qquad (104)$$

where $F_i^0=F_i/t^2$ and $N_i^0=N_i/t^2$, with F_i and N_i given in Tables I and II for $i=1-10$. In Eq. (104), when $i=1,\ldots 8$, $M_i(x)=\sum_f e_{q_f}^2\phi_{q_f/p}(x)$ is given by the twist-two quark distribution function in the proton,

$$\phi_{q_f/p}(x)\equiv\int\frac{dy^-}{2\pi}e^{ixP^+y^-}\left\langle A\left|\bar{\psi}_f(y^-)\frac{\not{n}}{2}\psi_f(0)\right|A\right\rangle . \qquad (105)$$

For $i=9,10$, $M_i(x)=(\sum_f e_{q_f}^2)[\phi_{g/p}(x)/x]$ is given by the twist-two gluon distribution function in the proton divided by x,

$$\frac{\phi_{g/p}(x)}{x}\equiv\int\frac{P^+dy^-}{2\pi}e^{ixP^+y^-}\langle A|A^\perp(y^-)A_\perp(0)|A\rangle . \qquad (106)$$

As in the case of twist-four, these leading-power cross sections for DIS can also be reduced to photoproduction straightforwardly.

For DIS, we shall present α for the differential cross section

$$\int d\phi_l E_l\frac{d\sigma}{dl^3dQ^2dx_B}=\pi\int d\phi\frac{Q^2}{wx_B^2}E_lE_{L'}\frac{d\sigma}{dl^3dL'^3}\ , \qquad (107)$$

where ϕ_l is the azimuthal angle of $l_\perp$, while ϕ is the relative azimuthal angle between $\mathbf{L'}_\perp$ and $l_\perp$. We choose the independent variables to be $l_\perp$, x_F, Q^2, and x_B, where $l_\perp$ and x_F depend on the momentum of the observed parton and Q^2 and x_B depend on the momentum of the final lepton. x_F and x_B are given explicitly by

$$x_F=-2l_3/\sqrt{s}\ ,\quad x_B=\frac{Q^2}{s+Q^2}\ . \qquad (108)$$

Note that in the kinematics of Sec. II, x_F is positive for a jet moving in the forward direction of the photon. In terms of $l_\perp$, x_F, Q^2, and x_B, the Mandelstam variable t has the form

$$t=-\frac{Q^2}{2x_B}\left\{\left[\frac{1-x_B}{x_B}\right]^{1/2}x_F+\left[\left[\frac{1-x_B}{x_B}\right]x_F^2+4\frac{l_T^2}{Q^2}\right]^{1/2}\right\}, \qquad (109)$$

which is useful for the computation.

Figures 6, 7, and 8 show α, calculated in the above manner for DIS at $Q^2=5$, 10, and 30 GeV^2, respectively, and at representative values of x_B. The beam energy used in our calculation is 470 GeV. Each graph shows α for $A\lambda^2=0.1$ GeV^2 (solid line) and 0.04 GeV^2 (dashed line). These two values were chosen to bracket the range of λ^2 suggested by data on dijet transverse momentum

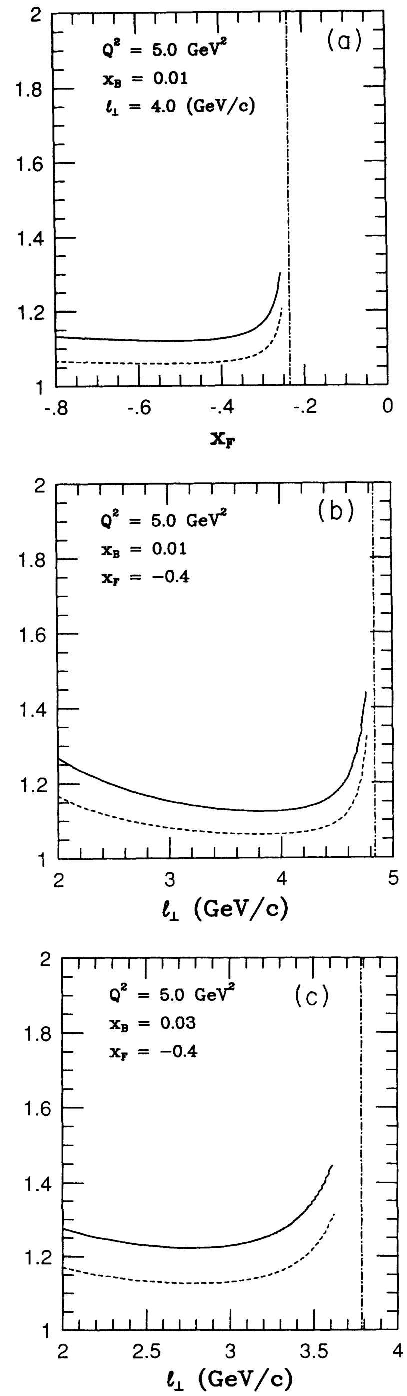

FIG. 6. Behavior of α, defined in Eq. (103), at $Q^2=5$ GeV^2. The dot-dashed line is the edge of phase space, i.e., $x_{\rm parton}=1.0$. The solid and dashed lines correspond to $\lambda^2=0.1$ and 0.04 GeV^2, respectively. (a) α as a function of x_F at $l_\perp=4.0$ GeV and $x_B=0.01$; (b) α as a function of $l_\perp$ at $x_F=-0.4$ and $x_B=0.01$; (c) α as a function of $l_\perp$ at $x_F=-0.4$ and $x_B=0.03$.

imbalance in photoproduciton [9,21]. The curves show the following general trends.

(i) α is generally in the range 1.1–1.3, depending on λ^2 and the kinematic variables.

(ii) α decreases mildly with $l_\perp$ at fixed x_F, followed by an increase near the edge of phase space, which is indicated in the figures by a vertical dot-dashed line.

(iii) α decreases with x_F at fixed $l_\perp$, again with an upturn near the edge of phase space.

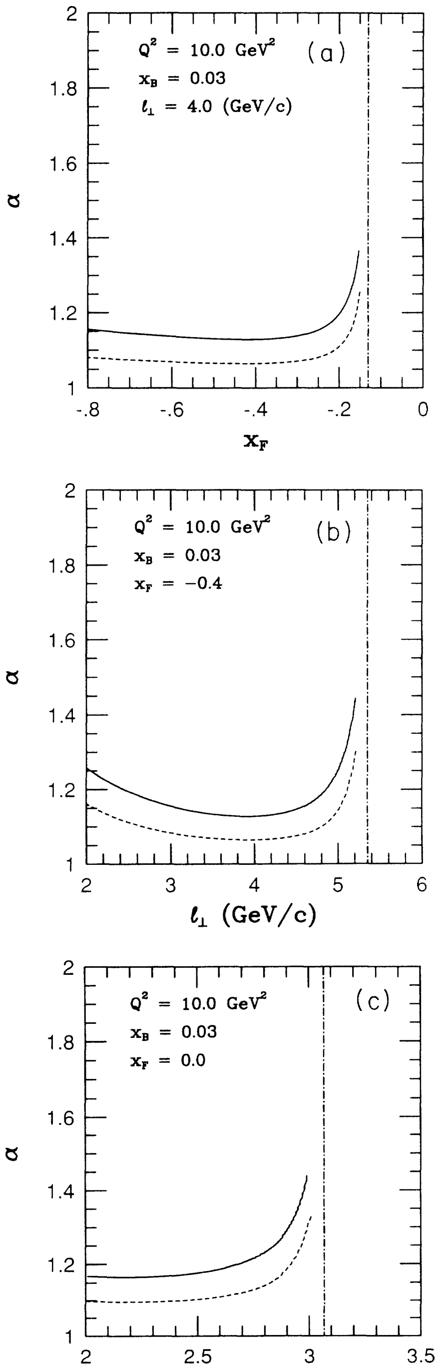

FIG. 7. Behavior of α, defined in Eq. (103), at $Q^2=10$ GeV^2. As in Fig. 6, the dot-dashed line is the edge of phase space, $x_{\text{parton}}=1.0$, and the solid and dashed lines correspond to $\lambda^2=0.1$ and 0.04 GeV^2, respectively. (a) α as a function of x_F at $l_\perp=4.0$ GeV and $x_B=0.03$; (b) α as a function of $l_\perp$ at $x_F=-0.4$ and $x_B=0.03$; (c) α as a function of $l_\perp$ at $x_F=0.0$ and $x_B=0.03$.

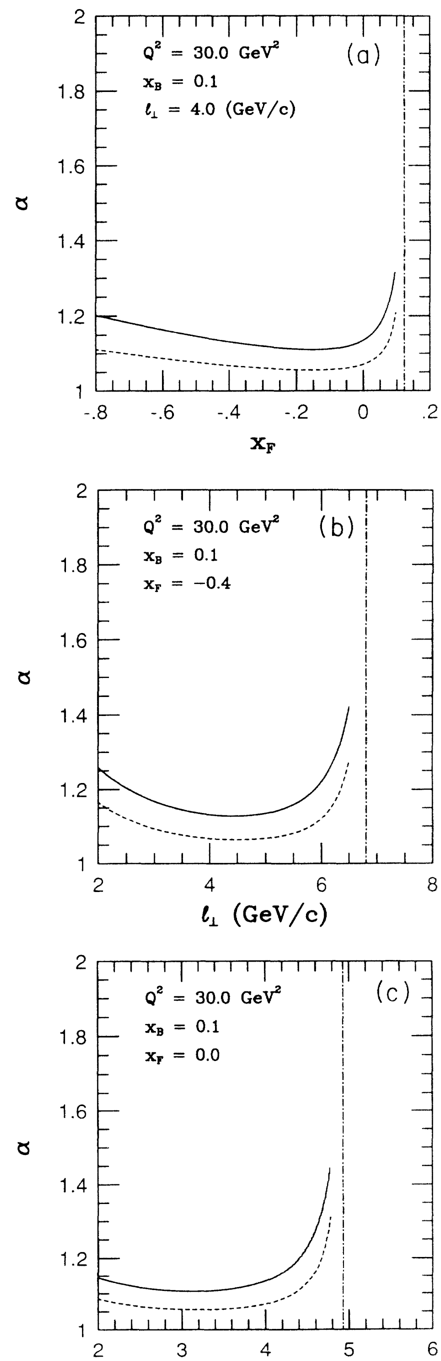

FIG. 8. Behavior of α, defined in Eq. (103), at $Q^2=30$ GeV^2. As in Fig. 6, the dot-dashed line is the edge of phase space, $x_{\text{parton}}=1.0$, and the solid and dashed lines correspond to $\lambda^2=0.1$ and 0.04 GeV^2, respectively. (a) α as a function of x_F at $l_\perp=4.0$ GeV and $x_B=0.1$; (b) α as a function of $l_\perp$ at $x_F=-0.4$ and $x_B=0.1$; (c) α as a function of $l_\perp$ at $x_F=0.0$ and $x_B=0.1$.

We may attribute the decrease with $l_\perp$ as an expected feature of a higher-twist process. The upturn at the edge of phase space comes from derivatives on the matrix elements $M_q(x)$ and $M_g(x)$ with respect to x in Eqs. (97) and (99).

We may note that $x = (-u)/(s+t+Q^2)$ is generically larger than $x_B = Q^2/(s+Q^2)$, and we do not expect shadowing to influence the main features of our results in the kinematic regions we show. Of course, in the larger context, the interplay of multiple scattering and shadowing is an interesting and challenging problem. Finally, we note that the double hard scattering contribution (Sec. V) is relatively small with the model matrix elements of Eq. (85c), giving a contribution to the cross section of the order of 10%.

The methods developed here can, we anticipate, be extended to other cross sections which exhibit nuclear enhancement. Progress in this direction is underway.

ACKNOWLEDGMENTS

We would like to express our appreciation for helpful and informative conversations and communications with Stan Brodsky, Geoff Bodwin, George Chang, Margorie Corchoran, Tom Fields, Lenny Frankfurt, Sean Gavin, Don Geesaman, Genya Levin, Joe Milana, Jorge Morfin, Gerry Miller, Donna Naples, Al Mueller, John Ralston, Mark Strikman, and Quan Zhu. This work was supported in part by the National Science Foundation under Grant No. PHY 9309888, the U.S. Department of Energy under Grants Nos. DE-FG02-87ER40731 and DE-FG02-92ER40730, and by the Texas National Research Laboratory.

[1] J. W. Cronin *et al.*, Phys. Rev. D **11**, 3105 (1975).

[2] B. Alper *et al.*, Phys. Lett. **44B**, 521 (1973); M. Banner *et al.*, *ibid.* **44B**, 537 (1973); F. W. Büsser *et al.*, *ibid.* **46B**, 471 (1973); J. W. Cronin *et al.*, Phys. Rev. Lett. **31**, 1426 (1973).

[3] A. S. Carroll *et al.*, Phys. Rev. Lett. **61**, 1698 (1988).

[4] L. Kluberg *et al.*, Phys Rev. Lett. **38**, 670 (1977); R. L. McCarthy *et al.*, *ibid.* **40**, 213 (1978); D. Antreasyan *et al.*, Phys. Rev. D **19**, 764 (1979); H. Jöstlein *et al.*, *ibid.* **20**, 53 (1979).

[5] D. M. Alde *et al.*, Phys Rev. Lett **64**, 2479 (1990); **66**, 133 (1991); **66**, 2285 (1991).

[6] C. Steward *et al.*, Phys. Rev. D **42**, 1385 (1990); A. Ziemminski, in *Proceedings of the Fourth Meeting of the Division of Particles and Fields of the American Physical Society,* Storrs, CT, edited by K. Haller *et al.* (World Scientific, Singapore, 1989), p. 672.

[7] M. D. Corcoran *et al.*, Phys. Lett. B **259**, 209 (1991); T. Fields, Nucl. Phys. **A544**, 565 (1992).

[8] M. Arneodo *et al.*, Nucl. Phys. **B333**, 1 (1990); P. Amaudruz *et al.*, Z. Phys. C **51**, 387 (1991); M. R. Adams *et al.*, Phys. Rev. Lett. **68**, 3266 (1992).

[9] D. Naples, in *Proceedings of the Seventh Meeting of the American Physical Society Division of Particles and Fields,* Fermi National Accelerator Laboratory, Batavia. IL, edited by C. H. Albright *et al.* (World Scientific, Singapore, 1993), p. 948.

[10] J. J. Ryan, in *Proceedings of the Seventh Meeting of the American Physical Society Division of Particles and Fields,* Fermi National Accelerator Laboratory, Batavia, IL, edited by C. H. Albright *et al.* (World Scientific, Singapore, 1993), p. 929.

[11] A. H. Mueller, in *Proceedings of the XVII Rencontre de Moriond,* Gif-sur-Yvette, edited by J. Tran Thanh Van (Editions Frontières, Gif-sur-Yvette, 1982), Vol. 1; S. J. Brodsky, in *Proceedings of the XIII International Symposium on Multiparticle Dynamics,* edited by E. W. Kittel, W. Metzger, and A. Stergiou (World Scientific, Singapore, 1982).

[12] A. H. Mueller and J. Qiu, Nucl. Phys. **B268**, 427 (1986); J. Qiu, *ibid.* **B291**, 746 (1987); L. Frankfurt and M. Strikman, Phys. Rep. **160**, 235 (1988); S. J. Brodsky and H. J. Lu, Phys. Rev. Lett. **64**, 1342 (1990); G. Piller and W. Weise, Phys. Rev. C **42**, 1834 (1990).

[13] P. M. Fishbane and J. S. Trefil, Phys. Rev. D **12**, 2113 (1975); J. H. Kühn, *ibid.* **13**, 2948 (1976); M. J. Longo, Nucl. Phys. **B134**, 70 (1978); A. Krzywicki, J. Engels, B. Petersson, and U. Sukhatme, Phys. Lett. **85B**, 407 (1979); V. V. Zmushko, Yad. Fiz. **32**, 246 (1980) [Sov. J. Nucl. Phys **32**, 127 (1980)].

[14] M. Lev and B. Petersson, Z. Phys. C **21**, 155 (1983); K. Kastella, G. Sterman, and J. Milana, Phys. Rev. D **39**, 2586 (1989).

[15] E. M. Levin and M. G. Ryskin, Yad. Fiz. **47**, 1397 (1988) [Sov. J. Nucl. Phys. **47**, 889 (1988)]; G. T. Bodwin, S. J. Brodsky, and G. P. Lepage, Phys. Rev. D **39**, 3287 (1989).

[16] M. Luo, J. Qiu, and G. Sterman, Phys. Lett. B **279**, 377 (1992).

[17] J. Qiu and G. Sterman, Nucl. Phys. **B353**, 105 (1991).

[18] J. Qiu and G. Sterman, Nucl. Phys. **B353**, 137 (1991).

[19] J. C. Collins, D. E. Soper, and G. Sterman, in *Perturbative Quantum Chromodynamics,* edited by A. H. Mueller (World Scientific, Singapore, 1989).

[20] R. K. Ellis, W. Furmanski, and R. Petronzio, Nucl. Phys. **B207**, 1 (1982); **B212**, 29 (1983); R. L. Jaffe, *ibid.* **B229**, 205 (1983).

[21] M. Luo, J. Qiu, and G. Sterman, Phys. Rev. D **49**, 4493 (1994).

[22] J. Qiu, Phys. Rev. D **42**, 30 (1990).

[23] R. Meng, F. I. Olness, and D. E. Soper, Nucl. Phys. **B371**, 79 (1992).

[24] Mueller and Qiu [12].

[25] J. Qiu and G. Sterman, Phys. Rev. Lett. **67**, 2264 (1991).